



## Measurements of reactive trace gases and variable O<sub>3</sub> formation rates in some South Carolina biomass burning plumes

S. K. Akagi<sup>1</sup>, R. J. Yokelson<sup>1</sup>, I. R. Burling<sup>1</sup>, S. Meinardi<sup>2</sup>, I. Simpson<sup>2</sup>, D. R. Blake<sup>2</sup>, G. R. McMeeking<sup>3</sup>, A. Sullivan<sup>3</sup>, T. Lee<sup>3</sup>, S. Kreidenweis<sup>3</sup>, S. Urbanski<sup>4</sup>, J. Reardon<sup>4</sup>, D. W. T. Griffith<sup>5</sup>, T. J. Johnson<sup>6</sup>, and D. R. Weise<sup>7</sup>

<sup>1</sup>University of Montana, Department of Chemistry, Missoula, MT 59812, USA

<sup>2</sup>Department of Chemistry, University of California-Irvine, Irvine, CA 92697, USA

<sup>3</sup>Colorado State University, Department of Atmospheric Science, Fort Collins, CO 80523, USA

<sup>4</sup>USDA Forest Service, Rocky Mountain Research Station, Fire Sciences Laboratory, Missoula, MT 59808, USA

<sup>5</sup>University of Wollongong, Department of Chemistry, Wollongong, New South Wales, Australia

<sup>6</sup>Pacific Northwest National Laboratories, Richland, WA 99354, USA

<sup>7</sup>USDA Forest Service, Pacific Southwest Research Station, Forest Fire Laboratory, Riverside CA 92507, USA

Correspondence to: R. J. Yokelson (bob.yokelson@umontana.edu)

Received: 5 September 2012 – Published in Atmos. Chem. Phys. Discuss.: 24 September 2012

Revised: 16 January 2013 – Accepted: 17 January 2013 – Published: 1 February 2013

**Abstract.** In October–November 2011 we measured trace gas emission factors from seven prescribed fires in South Carolina (SC), US, using two Fourier transform infrared spectrometer (FTIR) systems and whole air sampling (WAS) into canisters followed by gas-chromatographic analysis. A total of 97 trace gas species were quantified from both airborne and ground-based sampling platforms, making this one of the most detailed field studies of fire emissions to date. The measurements include the first emission factors for a suite of monoterpenes produced by heating vegetative fuels during field fires. The first quantitative FTIR observations of limonene in smoke are reported along with an expanded suite of monoterpenes measured by WAS including  $\alpha$ -pinene,  $\beta$ -pinene, limonene, camphene, 4-carene, and myrcene. The known chemistry of the monoterpenes and their measured abundance of 0.4–27.9 % of non-methane organic compounds (NMOCs) and  $\sim 21$  % of organic aerosol (mass basis) suggests that they impacted secondary formation of ozone (O<sub>3</sub>), aerosols, and small organic trace gases such as methanol and formaldehyde in the sampled plumes in the first few hours after emission. The variability in the initial terpene emissions in the SC fire plumes was high and, in general, the speciation of the initially emitted gas-phase NMOCs was 13–195 % different from that observed in a similar study in nominally similar pine forests in North Carolina  $\sim 20$  months earlier. It is likely that differences in stand struc-

ture and environmental conditions contributed to the high variability observed within and between these studies. Similar factors may explain much of the variability in initial emissions in the literature. The  $\Delta\text{HCN}/\Delta\text{CO}$  emission ratio, however, was found to be fairly consistent with previous airborne fire measurements in other coniferous-dominated ecosystems, with the mean for these studies being  $0.90 \pm 0.06$  %, further confirming the value of HCN as a biomass burning tracer. The SC results also support an earlier finding that C<sub>3</sub>–C<sub>4</sub> alkynes may be of use as biomass burning indicators on the time-scale of hours to a day. It was possible to measure the downwind chemical evolution of the plume on four of the fires and significant O<sub>3</sub> formation ( $\Delta\text{O}_3/\Delta\text{CO}$  from 10–90 %) occurred in all of these plumes within two hours. The slowest O<sub>3</sub> production was observed on a cloudy day with low co-emission of NO<sub>x</sub>. The fastest O<sub>3</sub> production was observed on a sunny day when the downwind plume almost certainly incorporated significant additional NO<sub>x</sub> by passing over the Columbia, SC metropolitan area. Due to rapid plume dilution, it was only possible to acquire high-quality downwind data for two other trace gas species (formaldehyde and methanol) during two of the fires. In all four of these cases, significant increases in formaldehyde and methanol were observed in  $< 2$  h. This is likely the first direct observation of post-emission methanol production in biomass burning plumes. Post-emission production of methanol does not

always happen in young biomass burning plumes, and its occurrence in this study could have involved terpene precursors to a significant extent.

## 1 Introduction

On a global scale, biomass burning is thought to be the largest source of primary fine carbonaceous particles in the atmosphere and the second largest source of total trace gases (Crutzen and Andreae, 1990; Bond et al., 2004; Akagi et al., 2011). In the southeastern US and to a lesser extent in other parts of the US and other countries, prescribed fires are ignited to restore or maintain the natural, beneficial role that fire plays in fire-adapted ecosystems (Biswell, 1989; Carter and Foster, 2004; Keeley et al., 2009). In addition, prescribed fires reduce wildfire risk and smoke impacts by consuming accumulated fuels under weather conditions when smoke dispersion can be at least partially controlled (Hardy et al., 2001; Wiedinmyer and Hurteau, 2010; Cochrane et al., 2012). On many southeastern US wildland sites, land managers will implement prescribed burning every 1–4 yr under conditions where fuel consumption is expected only in understory fuels and the forecast transport is such that smoke impacts will be minimized. However, despite land managers' best efforts, prescribed fires, along with wildfires, do impact local-to-regional air quality (ozone, O<sub>3</sub>; particulate matter, PM), health, and visibility in the southeastern US and elsewhere (McMeeking et al., 2006; Pfister et al., 2006; Park et al., 2007; Liu et al., 2009). Thus, optimizing land-use strategies for ecosystem health, climate, and air quality requires detailed knowledge of the chemistry and evolution of smoke (Rappold et al., 2011; Roberts et al., 2011; Akagi et al., 2012).

The work reported here is the last field deployment in a series of measurements of prescribed fire emissions from the southeastern US (Burling et al., 2010, 2011; Yokelson et al., 2013). The major features of this study were to expand the scope of measurements to include: (1) emissions data for fires that burned in forest stands with a broader range of management histories, as well as in additional important fuel types, (2) post-emission plume evolution data on days with different solar insolation and on a day with significant mixing of urban and fire emissions, and (3) addressing all these topics with a significantly expanded suite of instrumentation. The previous pine-forest understory fire measurements in this overall study had been made in coastal North Carolina (NC) in February and March of 2010 after a prolonged period of high rainfall in intensively managed loblolly pine (*Pinus taeda*) and longleaf pine (*Pinus palustris*) stands (Burling et al., 2011). More specifically, the units had been treated with prescribed fire, mechanical fuel reduction, or logged within the last 1–5 yr so that the understory reflected less than five years of re-growth. Through collabo-

ration with the US Army's Fort Jackson (FJ) in the Sandhills region of South Carolina, we were able to sample emissions from pine-forest understory fires in longleaf pine stands that had not been logged or burned by wild or prescribed fires in over 50 yr. The lower historical frequency of disturbance factors contributed to denser stands with relatively more hardwoods, litter, and shrubs in the understory fuels. Further, the fires reported here occurred during the 2011 fall prescribed fire season before the region had fully recovered from a prolonged summer drought. Thus, this study significantly increased the range of germane fuel and environmental conditions for which prescribed fire emissions have been measured. Plume evolution data could not be acquired during the spring 2010 prescribed fire measurements in pine-forest understory fires, due primarily to air-space restrictions. In contrast, in this study we had access to the downwind plume for four of seven fires and measured photochemical changes on one day with thick cloud cover and on three days with high solar insolation that included one day when the fire emissions mixed with the urban plume from the Columbia, SC metropolitan area.

The suite of instruments was significantly expanded for the final field deployment reported here. The early spring 2010 emissions data were produced by airborne and ground-based Fourier transform infrared spectrometers (AFTIR and LAFTIR, respectively) and an airborne nephelometer to estimate PM<sub>2.5</sub> (particulate matter < 2.5 microns in diameter, Burling et al., 2011). In the work reported here, the trace gas measurements were supplemented by whole air sampling (WAS) on the ground and in the air. The particulate measurements featured a large suite of instruments to be described in detail in companion publications (McMeeking et al., 2013). Here we report the measurements obtained by AFTIR, LAFTIR, and WAS, which sampled trace gases in either well-lofted or initially unlofted emissions. Initial emissions are discussed first followed by observations in the aging plumes.

## 2 Experimental details

### 2.1 Airborne Fourier transform infrared spectrometer (AFTIR)

The AFTIR on the Twin Otter was similar in concept to AFTIR instruments flown from 1997–2010 and described elsewhere (Yokelson et al., 1999; Burling et al., 2011). However, the 2011 version of the AFTIR featured several hardware changes including the deployment of a Bruker Matrix-M IR Cube FTIR spectrometer. The FTIR was operated at a spectral resolution of 0.67 cm<sup>-1</sup> (slightly lower than 0.5 cm<sup>-1</sup> used previously) and four spectra were co-added every 1.5 s with a duty cycle > 95 %. The f-matched exit beam from the FTIR was directed into a closed-path doubled White cell (IR Analysis, Inc.) permanently aligned at 78 m. The exit beam

from the cell was focused onto a mercury cadmium telluride (MCT) detector. A forward-facing halocarbon wax coated inlet (25 mm i.d.) opening 30 cm above the top of the leading edge of the aircraft cabin ceiling directed ram air into a 25 mm diameter perfluoroalkoxy (PFA) tube coupled to the White cell. The noise level for the four co-added spectra was  $4 \times 10^{-4}$  absorbance units, which allowed CO and CH<sub>4</sub> to be measured in near “real time” with about 3–5 ppb peak-to-peak noise. Peak-to-peak noise for CO<sub>2</sub> operating in this manner was about 1 ppm. The temporal resolution with the valves open was limited by the cell 1/e exchange time of about 5–10 s at typical Twin Otter sampling speeds of  $\sim 40$ – $80 \text{ m s}^{-1}$ . Fast-acting, electronically activated valves located at the cell inlet and outlet allowed flow through the cell to be temporarily halted so that more scans of “grab samples” could be averaged to increase sensitivity. Averaging  $\sim 100$  scans (150 s) of a “grab sample” reduced peak-to-peak noise to  $3 \times 10^{-5}$  absorbance units, providing, for example, a methanol detection limit better than  $\sim 400$  pptv (signal-to-noise ratio, SNR = 1). At times we averaged scans obtained with the control valves open, which gave SNRs dependent on the time to transect the plume. AFTIR sensitivity is also impacted by interference from water vapor, which is highly variable. In general the sensitivity has improved up to a factor of  $\sim 30$  depending on the spectral region, since the first prototype AFTIR system was flown in 1997–2006. Detection limits for the compounds we report other than CO<sub>2</sub> (see below) ranged from hundreds of ppt to 10 ppb for NO and NO<sub>2</sub>, where the gain in SNR was partially canceled by the decreased resolution.

The averaged sample spectra were analyzed either directly as single-beam spectra, or as transmission spectra referenced to an appropriate background spectrum, via multi-component fits to selected frequency regions with a synthetic calibration non-linear least-squares method (Griffith, 1996; Yokelson et al., 2007; Burling et al., 2011). The fits utilized both the HITRAN (Rothman et al., 2009) and Pacific Northwest National Laboratory (Johnson et al., 2006, 2010) spectral databases. As an exception to the fitting process, NO and NO<sub>2</sub> only were analyzed by integration of selected peaks in the absorbance spectra. In all, the following gases were quantified and accounted for most of the features observed in the smoke spectra: water vapor (H<sub>2</sub>O), carbon dioxide (CO<sub>2</sub>), carbon monoxide (CO), methane (CH<sub>4</sub>), nitric oxide (NO), nitrogen dioxide (NO<sub>2</sub>), ammonia (NH<sub>3</sub>), hydrogen cyanide (HCN), nitrous acid (HONO), peroxy acetyl nitrate (PAN, CH<sub>3</sub>C(O)OONO<sub>2</sub>), ozone (O<sub>3</sub>), glycolaldehyde (HOCH<sub>2</sub>CHO), ethylene (C<sub>2</sub>H<sub>4</sub>), acetylene (C<sub>2</sub>H<sub>2</sub>), propylene (C<sub>3</sub>H<sub>6</sub>), limonene (C<sub>10</sub>H<sub>16</sub>), formaldehyde (HCHO), 1,3-butadiene (C<sub>4</sub>H<sub>6</sub>), methanol (CH<sub>3</sub>OH), furan (C<sub>4</sub>H<sub>4</sub>O), phenol (C<sub>6</sub>H<sub>5</sub>OH), acetic acid (CH<sub>3</sub>COOH), and formic acid (HCOOH). The spectral retrievals were almost always within 1 % of the nominal values for a series of NIST-traceable standards of CO<sub>2</sub>, CO, and CH<sub>4</sub> with accuracies between 1 and 2 %. For NH<sub>3</sub> only, we corrected for losses on the cell walls

as described in Yokelson et al. (2003a). The excess mixing ratios for any species “X” in the plumes (denoted  $\Delta X$ , the mixing ratio of species “X” in a plume minus its mixing ratio in background air) were obtained directly from the absorbance or transmission spectra retrievals or by difference between the appropriate single beam retrievals for H<sub>2</sub>O, CO<sub>2</sub>, CO, and CH<sub>4</sub>.

## 2.2 Land-based Fourier transform infrared spectrometer (LAFTIR)

Ground-based FTIR measurements were made using our battery-powered FTIR system (Christian et al., 2007) that can be wheeled across difficult terrain to sample remote sites. The vibration-isolated LAFTIR optical bench holds a MIDAC 2500 spectrometer, an MCT detector, and a White cell (Infrared Analysis, Inc.) aligned at 11.35 m pathlength. Sample air was drawn into the cell by an onboard pump through several meters of 0.635 cm o.d. corrugated PFA tubing. Two manual PFA shutoff valves allowed trapping of the sample in the cell to collect signal averaged spectra. Temperature and pressure inside the White cell were monitored and logged in real time on the on-board system laptop. Several upgrades to the FTIR originally described by Christian et al. (2007) included improvements to the electronics, source optics, and the data acquisition software (Essential FTIR, <http://www.essentialftir.com/index.html>). The LAFTIR was operated at  $0.50 \text{ cm}^{-1}$  and three scans were co-added every 1.15 s (with a duty cycle of about 38 %). Smoke or background samples were typically held in the cell for several minutes while  $\sim 100$ – $200$  spectra were collected at  $\sim 1 \text{ Hz}$ . The spectral quantification method was similar to that used in the AFTIR analysis. Signal averaged, grab sample, single beam spectra were analyzed directly for H<sub>2</sub>O, CO<sub>2</sub>, CO, and CH<sub>4</sub> and referenced to appropriate background spectra to analyze for the following gases: NH<sub>3</sub>, HCN, C<sub>2</sub>H<sub>2</sub>, C<sub>2</sub>H<sub>4</sub>, C<sub>3</sub>H<sub>6</sub>, HCHO, CH<sub>3</sub>OH, CH<sub>3</sub>COOH, C<sub>6</sub>H<sub>5</sub>OH, C<sub>4</sub>H<sub>4</sub>O, C<sub>10</sub>H<sub>16</sub>, and C<sub>4</sub>H<sub>6</sub>. We corrected for NH<sub>3</sub> losses on the White cell walls during storage, which increased the LAFTIR NH<sub>3</sub> retrievals in this study by about 40 % on average (Yokelson et al., 2003a). Due mostly to a shorter pathlength (compared to the AFTIR system, see previous section), the LAFTIR detection limits ranged from  $\sim 50$ – $200$  ppb for most gases. This was sufficient for detection of many species since much higher concentrations were sampled on the ground than in the lofted smoke. Comparisons to the NIST-traceable standards for CO, CO<sub>2</sub>, and high levels of CH<sub>4</sub> were usually within 1–2 %. Background level calibrations for CH<sub>4</sub> had weaker signals and up to 6 % uncertainty but that does not introduce significant error into the excess amounts in most cases. Several compounds observed by the AFTIR system (formic acid, glycolaldehyde, PAN, O<sub>3</sub>, NO, NO<sub>2</sub>, and HONO) were below the detection limits of the ground-based system. Finally, in several LAFTIR spectra a prominent peak was seen at  $882.5 \text{ cm}^{-1}$  that we could not assign.

### 2.3 Whole air sampling (WAS) canisters

WAS canisters were filled both on the ground and from the Twin Otter to measure an extensive suite of gases, mostly non-methane organic compounds (NMOCs), as described in detail elsewhere (Simpson et al., 2011). Sampling was manually controlled and the evacuated canisters were filled to ambient pressure in  $\sim 10$ – $20$  s in background air or in various smoke plumes. On the ground, the WAS samples were obtained in more dilute portions of the plumes than sampled by LAFTIR since the subsequent pre-concentration step could otherwise cause a non-linear detector response (Hanst et al., 1975; Simpson et al., 2011). In the aircraft, the canisters were filled directly from the AFTIR multipass cell via a dedicated PFA valve and connecting tube after the IR signal averaging was complete. We collected four WAS canisters from the ground and four from the air (one background and three smoke samples per platform per fire) on each of the first three fires (Block 6, Block 9b, and Block 22b, see Sect. 2.6). All but one WAS sample was collected in fresh smoke with depleted O<sub>3</sub> (see Sect. 3.7) and all WAS samples were analyzed for 89 gases within 2–5 days of collection (to minimize potential loss or growth of certain analytes within the canisters; see Simpson et al., 2011). CO<sub>2</sub>, CH<sub>4</sub>, CO, carbonyl sulfide (OCS), dimethyl sulfide (DMS), and 83 NMOCs were quantified using gas chromatography (GC) coupled with flame ionization detection (FID), electron capture detection (ECD), and quadrupole mass spectrometer detection (MSD). Every peak of interest on every chromatogram was individually inspected and manually integrated. The GC run times were extended to target quantification of limonene. Other prominent peaks in the chromatograms were observed, assigned, and quantified for species not in the suite of compounds usually analyzed by UC-Irvine, including 2-propenal (acrolein), 2-methylfuran and butanone. Additional details on WAS preparation, technical specifications, and analysis protocols can be found in Simpson et al. (2011).

### 2.4 Other airborne measurements

In addition to the AFTIR and WAS measurements, several other airborne instruments were part of this campaign, including a single particle soot photometer (SP2) for measurement of refractory black carbon at STP (rBC,  $\mu\text{g sm}^{-3}$ , 273 K, 1 atm) (Stephens et al., 2003), a particle-into-liquid sampler-total organic carbon (PILS-TOC, Weber et al., 2001) analyzer to detect water-soluble organic carbon (WSOC), and a high resolution time-of-flight (HR-ToF) aerosol mass spectrometer (AMS) to measure the mass concentration ( $\mu\text{g sm}^{-3}$ ) for the major non-refractory particle species including organic aerosol (OA), non-sea salt chloride, nitrate, sulfate, and ammonium. The AMS has been described in full detail elsewhere (Drewnick et al., 2005; Canagaratna et al., 2007). A Picarro cavity ring-down spectrometer measured H<sub>2</sub>O, CO<sub>2</sub>, CO, and CH<sub>4</sub> at 0.5 Hz during flight, and used

the same sampling inlet as the particle instruments. The particle/Picarro inlet was located adjacent to the AFTIR inlet and the Picarro was calibrated inflight with the same standards used to characterize the AFTIR retrievals. Thus, ratiating the particle data to the Picarro CO measurements allowed accurate synthesis of the particle data with the AFTIR and WAS trace gas measurements on the aircraft following procedures explained in detail elsewhere (Yokelson et al., 2009). Measurements of the aircraft position, ambient three-dimensional wind velocity, temperature, relative humidity, and barometric pressure at 1-Hz were obtained with a wing-mounted Aircraft Integrated Meteorological Measuring System probe (AIMMS-20, Aventech Research, Inc.) (Beswick et al., 2008).

### 2.5 Calculation of excess mixing ratios, normalized excess mixing ratios (NEMRs), emission ratios (ERs), and emission factors (EFs)

Excess mixing ratios for FTIR species were calculated following the procedure in Sect. 2.1. Excess mixing ratios for WAS species were obtained by subtracting WAS background values from WAS plume values. The normalized excess mixing ratio (NEMR) is calculated for all instruments by dividing  $\Delta X$  by the excess mixing ratio of a long lived plume “tracer”  $\Delta Y$ , usually  $\Delta\text{CO}$  or  $\Delta\text{CO}_2$ , measured in the same sample as “X.” The NEMR can be measured anywhere in the plume. NEMRs collected at the source of a fire are equivalent to an initial molar emission ratio (ER) at the time of measurement. The ER has two important uses: (1) since the CO or CO<sub>2</sub> tracers dilute at the same rate as the other species, differences between the ERs and the NEMRs measured downwind can sometimes allow us to quantify post-emission chemical changes (for applicable conditions see Sect. 3.7). (2) The ERs can be used to calculate emission factors (EFs). Details of these two uses are described below.

In this study, downwind data were only collected in the aircraft and the ER obtained while the aircraft was sampling the source did not follow clear, time-dependent trends. Thus we combined all the source samples from each fire to compute a single fire-averaged initial emission ratio (and 1- $\sigma$  standard deviation) for each fire. The fire-averaged ER were subsequently used both to calculate fire-averaged EF and as our best estimate of the starting conditions in the plumes. We computed the fire-averaged ERs from the slope of the linear least-squares line with the intercept forced to zero when plotting  $\Delta X$  against  $\Delta Y$  (Yokelson et al., 1999) for all X/Y pairs from the fire. The intercept is forced to zero because the background concentration is typically well known and variability in the plume can affect the slope and intercept if the intercept is not forced. This method heavily weights the large excess mixing ratios that may reflect higher rates of fuel consumption and data that have higher signal-to-noise. FTIR and WAS excess mixing ratios were combined in the calculation

**Table 1.** Fire name, location, date, fuels description, size, atmospheric conditions, and burn history of fires sampled in this work.

Fire Name	Location	Date (2011)	Fuel Description	Area Burned (ha)	Temperature (° C)	Relative Humidity (%RH)	Windspeed (m s <sup>-1</sup> )	Atmospheric Conditions	Stand History	Latitude (° N)	Longitude (° W)
Block 6	Fort Jackson, SC	30 Oct	Block 6, mature long leaf pine	61.9	8–16	64	3–5	3.6 mm rain previous morning	Last burned 1957	34°1'29"	80°52'16"
Block 9b	Fort Jackson, SC	1 Nov	Block 9b, mature long leaf pine, sparkleberry	36.0	9–18	58–69	3–4	Mixing height ~1650 m. Clear skies	Last burned 1956	34°0'15"	80°52'37"
Block 22b	Fort Jackson, SC	2 Nov	Block 22b, mature long leaf and loblolly pine and oak	28.7	13–18	~70 (avg)	2–3	Clear, Mixing height 1160 m.	Last burned 2003	34°5'4"	80°46'23"
Pine Plantation	Orangeburg County, SC	2 Nov	Plantation fire, loblolly pine debris	16.2	~19	~71 (avg)	2–3	Sunny/clear	unk*	33°34'49"	81°9'55"
Georgetown	Georgetown, SC	7 Nov	SC coastal grass understory fire	60.7	20–22	~74 (avg)	4–4.5	Sunny/clear	unk	33°12'9"	79°24'6"
Francis Marion	Francis Marion National Forest, SC	8 Nov	Longleaf pine, wiregrass	147	19–21	~83 (avg)	0.5–3	Sunny/clear	unk	33°12'55"	79°28'34"
Bamberg	Midway, SC	10 Nov	Longleaf/loblolly pine understory	36.4	16–21	~71 (avg)	2–3	Cloudy with rain at end of flight	unk	33°14'5"	80°56'41"

\* “unk” indicates that the date of the last previous fire on the site is unknown.

of ERs if a species was measured by both techniques (see Sect. 3.1).

For any carbonaceous fuel, source ERs can be used to calculate emission factors (EFs), which are expressed as grams of compound emitted per kilogram of biomass burned (on a dry weight basis). A set of ERs obtained at any point during the fire could be used to calculate a set of EFs relevant to the time of the sample. For this study, however, we use the fire-averaged ERs (obtained as described above) to calculate a single set of fire-averaged EFs for each fire using the carbon mass-balance method (Yokelson et al., 1996, 1999), shown below (Eq. 1):

$$EF(\text{g kg}^{-1}) = F_C \times 1000 \times \frac{MM_X}{MM_C} \times \frac{C_X}{C_T} \quad (1)$$

where  $F_C$  is the mass fraction of carbon in the fuel,  $MM_X$  is the molecular mass of compound  $X$ ,  $MM_C$  is the molecular mass of carbon (12.011 g mol<sup>-1</sup>), and  $C_X/C_T$  is the number of emitted moles of compound  $X$  divided by the total number of moles of carbon emitted. This method is most accurate when the mass fraction of carbon in the fuel is precisely known and all the burnt carbon is volatilized and detected. Based on literature values for similar fuels (Susott et al., 1996; Burling et al., 2010) we assumed a carbon fraction of 0.50 by mass on a dry weight basis for fuels burned in this campaign. The actual fuel carbon fraction was likely within 5–10 % of this value. Note that EFs scale linearly with

the assumed fuel carbon fraction. Total emitted carbon in this study was determined from the sum of the carbon from AF-TIR species and WAS species. This sum could underestimate the actual total carbon by 1–2 % due to unmeasured carbon, which would lead to a slight, across-the-board overestimate of our calculated EFs of 1–2 % (Akagi et al., 2011).

Because the emissions from flaming and smoldering processes differ, we use the modified combustion efficiency, or MCE, to describe the relative contribution of each of these combustion processes, where higher MCEs indicate more flaming combustion (Ward and Radke, 1993; Yokelson et al., 1996) (Eq. 2):

$$\text{MCE} = \frac{\Delta\text{CO}_2}{\Delta\text{CO}_2 + \Delta\text{CO}} \quad (2)$$

## 2.6 Site descriptions

For each of the seven prescribed fires sampled in this study, the fuels, weather, size, location, etc. are shown in Table 1. The three prescribed fires of 30 October, 1 November, and 2 November 2011 (referred to as Blocks 6, 9b, and 22b, respectively) were located on the US Army's Fort Jackson base northeast of Columbia, SC. Blocks 6, 9b, and 22b were last burned in 1957, 1956, and 2003, respectively. The overstory vegetation consisted primarily of mature southern pines, including longleaf pine and loblolly pine. High density pine areas had high canopy closure and limited understory

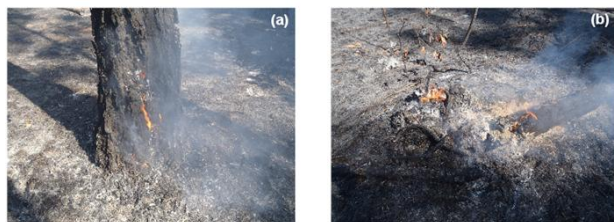


**Fig. 1.** Photographs of two examples of the fuels that contributed to residual smoldering combustion emissions that were sampled by ground-based FTIR and WAS: (a) a live tree base, and (b) dead/down debris.

vegetation with a thick litter layer (mostly pine needles). Lower density pine areas had turkey oak (*Quercus laevis* Walter) and other deciduous and herbaceous vegetation (i.e. grasses) as significant components of the understory. Farkleberry (*Vaccinium arboreum* Marsh.), also known as sparkleberry, was present in significant quantities intermixed with mature pine in Block 9b.

## 2.7 Airborne and ground-based sampling approach

The Fort Jackson prescribed burns (Blocks 6, 9b, and 22b) were part of a collaboration with the forestry staff at the base. The LAFTIR ground-based sampling protocol was similar to that described in Burling et al. (2011). Background samples were acquired before the fire and the burns were ignited in the late morning or early afternoon. Ground-based sampling access was sometimes precluded during ignition, but sampling access then continued through late afternoon until each fire was effectively out. During post-ignition access, numerous point sources of residual smoldering combustion (RSC) smoke were sampled by the mobile LAFTIR system minutes to hours after passage of a flame front. The spot sources of white smoke, mainly produced from pure smoldering combustion, included smoldering stumps, fallen logs, duff layers, etc., and they contributed to a dense smoke layer usually confined below the canopy. Point sources were usually sampled repeatedly to quantify their variability. Four WAS canisters were collected on the ground for each Fort Jackson fire (one WAS canister was always collected prior to ignition as a background along with three sampled RSC point sources, also sampled by the LAFTIR system). Table 2 shows the RSC fuel types sampled on the ground for the Fort Jackson fires and Fig. 1 illustrates two of these fuels.

For the airborne measurements, mid-morning take-offs enabled us to sample the pre-fire background and then the initial emissions and adjacent backgrounds for as long as the fire produced a convection column that exceeded several hundred meters in height. To measure the initial emissions from the fires, we sampled smoke less than several minutes old by penetrating the smoke column 150 to several thousand meters from the flame front. The goal was to sample

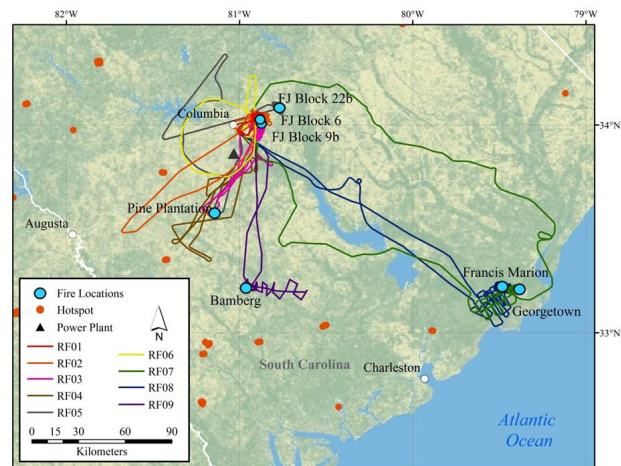


**Fig. 2.** Overview of all flight tracks for the Twin Otter aircraft from this campaign. “RF” indicates research flight and the dates of each research flight are shown in Table 3 except for RF06, which sampled urban emissions only on 5 November “Hotspots” are the MODIS thermal anomalies from 30 October to 10 November 2011. Of the seven fires sampled in this study, only the pine plantation fire was detected as a satellite hotspot. Due to a GPS malfunction, the 10 November flight track is at 2-min resolution retrieved from the USFS automated flight following system.

smoke that had already cooled to the ambient temperature since any chemical changes associated with smoke cooling are not explicitly included in most atmospheric models. This approach also sampled smoke before most photochemical processing, which is explicitly included in most models. Afternoon flights were conducted to complete sampling of the initial emissions if necessary and to search for and sample the downwind plume (Figs. 2, 3, and 4). The plumes diluted rapidly mostly in the top half of the already-polluted boundary layer due to brisk, shifting transport winds (4–10 m s<sup>-1</sup>) and strong vertical mixing (unstable atmosphere with the mixed layer extending to ~1100–1600 m above mean sea level, a.m.s.l.). Thus, of the Fort Jackson fires, it was only possible to locate the downwind plume and obtain quality downwind data on the Block 9b fire (1 November, research flights number 3 and 4; RF03 and RF04 in Fig. 3, respectively). The prevailing winds on 1 November directed the plume through the Columbia metropolitan area and directly over an airport and a natural gas power plant; thus mixing of burn smoke with fossil fuel emissions was unavoidable. The plume from the Block 22b fire directly entered a large restricted area and could not be subsequently re-sampled. However, while searching for the downwind plume we located a fire on a pine plantation about 40 km south of Columbia (Table 1). The Pine Plantation fire generated a Geostationary Satellite System (GOES) hotspot from 13:02:00–17:15:00 LT, so our samples at ~16:42 LT were collected towards the end of this fire. This was the only fire in this study detected as

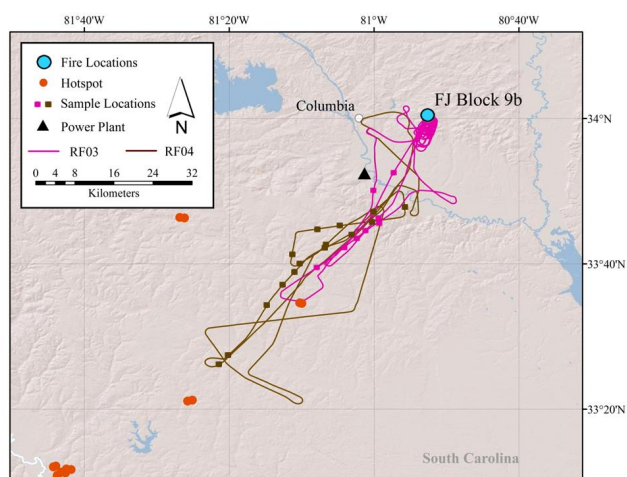


**Fig. 3.** Detailed flight tracks and AFTIR downwind sample locations during RF03 (pink) and RF04 (brown), which sampled the Block 9b fire at Fort Jackson on 1 November 2011. (The hotspot that appears to intersect RF03 is actually from the pine plantation fire sampled on 2 November.)

a hotspot by GOES or Moderate Resolution Imaging Spectroradiometer (MODIS) satellites.

After the burns at Fort Jackson, we sampled additional fires throughout South Carolina on 7, 8, and 10 November (Georgetown, Francis Marion, and Bamberg Fires, respectively). Due to transit time the Twin Otter typically arrived after the fire had been in progress for 0.5 to 1.0 h (ground-based sampling was not feasible due to long travel times and short notice). The airborne sampling of these fires initially focused on the source emissions. After  $\sim 1$ –1.5 h of repeatedly sampling the source, we would then cross the plume at increasingly large downwind distances until it could not be differentiated from background air. We then repeated the crossing pattern in reverse order or returned directly to the source approximately along the plume center-line depending on conditions (Fig. 4). The plumes from these three fires diluted rapidly, like the Fort Jackson plumes for similar reasons, and formed broad “cone-shaped” plumes in the boundary layer. Estimated times since emission, or smoke “ages”, were calculated for all the downwind samples by first calculating the average wind speed from the AIMMS-20 for incremental altitude bins of 100 m a.m.s.l. The smoke sample distance from the plume source was then divided by the average wind speed at the sample altitude, as shown in Eq. (3). The majority of the uncertainty is in the wind speed variability, which was typically  $\sim 28\%$ .

$$\text{Time Since Emission} = \frac{\text{Sample distance from source (m)}}{\text{Wind speed (at sample altitude, m s}^{-1}\text{)}} \quad (3)$$

**Table 2.** Ground-based fuels sampled by LAFTIR and WAS from Blocks 6, 9b, and 22b at Fort Jackson, SC.

Fuel Type	# of Sites	# of LAFTIR Samples	# of WAS Samples
Dead/down debris	8	13	3
Stump	4	4	2
Live tree base	2	5	–
Duff/Litter	4	4	–
Fatwood	2	6	1
Slash pile	1	4	–

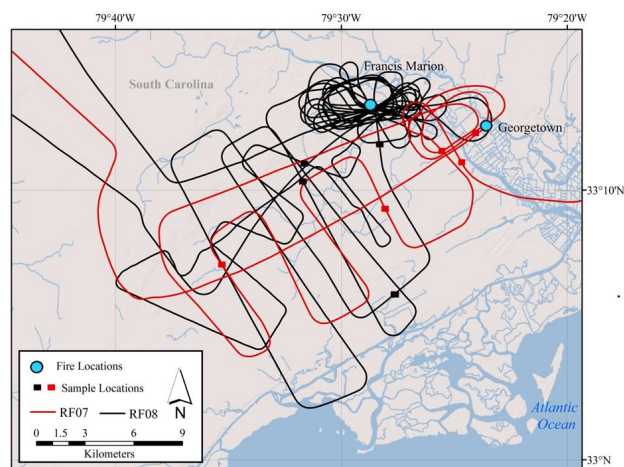


**Fig. 4.** Detailed flight tracks and AFTIR downwind sample locations during RF07 (red) and RF08 (black) on 7 and 8 November, sampling the Georgetown and Francis Marion fires, respectively.

### 3 Results and discussion

#### 3.1 Initial emissions

As mentioned above, FTIR and WAS samples were combined in the calculation of fire-average emission ratios for species measured by both techniques from airborne and ground-based platforms. Good agreement (within 20 %) was observed when ERs were calculated by each technique independently (Fig. 5a, b). The majority of ER plots show strong correlation with CO as the reference species. However, the LAFTIR ground-based measurements showed greater scatter compared to airborne measurements, because the individual contributions from different fuel elements were measured separately rather than blended together in a convection column (Bertschi et al., 2003). This increased scatter simply reflects real variability and not a decreased quality in the measurement of ERs. Additionally, the  $\text{ER}(\Delta\text{CH}_4/\Delta\text{CO})$  calculated from LAFTIR ground measurements is a factor of 3 higher than that from airborne measurements, which is well within the variability that we routinely observe for this ratio (Burling et al., 2011). Rather than attempting to assign

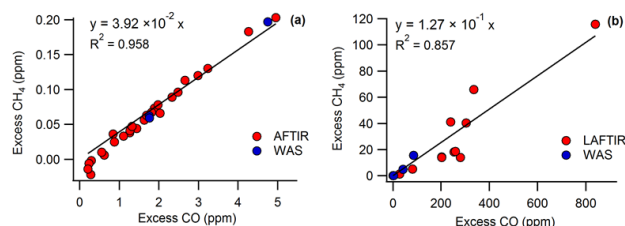


**Fig. 5.** Emission ratio plots of  $\Delta\text{CH}_4/\Delta\text{CO}$  from (a) the airborne FTIR multipass cell and (b) independent RSC targets on the ground (LAFTIR) from Blocks 6 and 9b, respectively. Red circles denote samples collected by FTIR and blue circles denote samples that were collected by WAS on the indicated fires.

this variability to specific factors, our main goal was to use these data to help characterize the full range of variability in fire emissions. The fire-averaged and platform-based study average emission factors for all species measured are shown in Table 3. Measurements were obtained from both airborne and ground-based platforms for all Fort Jackson fires (Blocks 6, 9b, and 22b). Only airborne data were collected for the remaining four fires. WAS cans were collected for the Fort Jackson burns and the 2 November Pine Plantation burn. Organic aerosol (OA) was measured by the AMS for five of the seven fires, and detailed AMS results will be presented in a complementary work (McMeeking et al., 2013). Up to 97 trace gas species were quantified by FTIR and WAS from both airborne and ground-based platforms, possibly the most comprehensive suite of trace gas species measured in the field for biomass burning fires to date.

Emission factors for most species depend on the flaming to smoldering ratio, or MCE, and for this reason Table 4 shows linear regression statistics of EFs as a function of MCE for all fires sampled in this study. A negative slope denotes higher EF at lower MCE and that the compound is likely emitted by smoldering combustion (e.g. CH<sub>3</sub>OH). Conversely, a positive slope, indicating higher EF with increasing MCE, is normally observed for compounds produced mainly by flaming combustion (e.g. NO<sub>x</sub>). Some species show poor correlation with MCE, indicating that other factors are dominating the variability in EF (e.g. phenol). Differences in fuel composition (e.g. %N) can also mask the dependence of EFs on MCE (Bertschi et al., 2003; Christian et al., 2007; McMeeking et al., 2009; Burling et al., 2010). Additionally, some compounds can be emitted by both flaming and smoldering combustion, such as C<sub>2</sub>H<sub>2</sub>. Ethyne showed a strong positive correlation with MCE in Yokelson et al. (2008) but a weak positive correlation with MCE in this work and in Burling et al. (2011), while other studies (Burling et al., 2010; Yokelson et al., 2011) report a weak negative correlation with MCE. Numerous variables affect emissions and the predictive power of any one variable or small group of variables is limited.

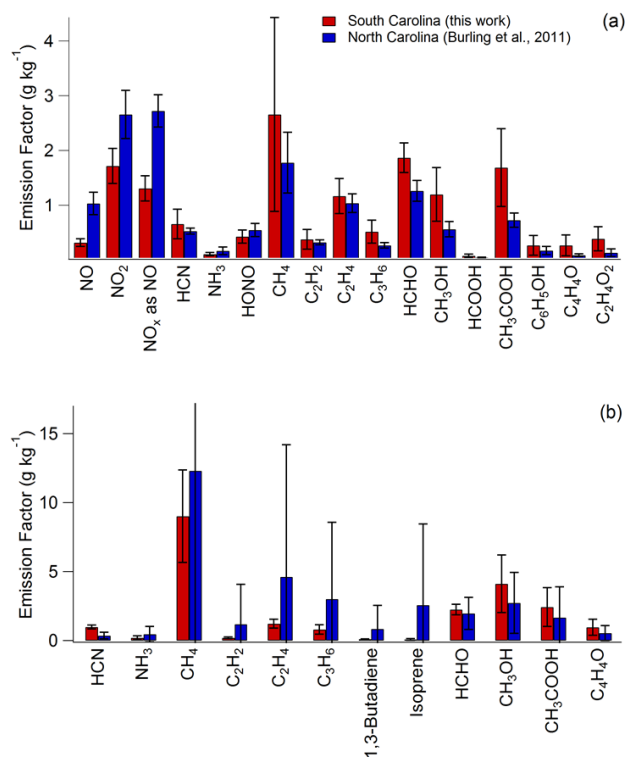


**Fig. 6.** Comparison of emission factors from this work (red) with Burling et al. (2011) (blue) from (a) airborne and (b) ground-based platforms.

### 3.2 Brief comparison to similar work

It is of interest to compare both the airborne and ground-based emission factors in this work to the EFs from the North Carolina coastal fires of Burling et al. (2011) (Fig. 6). In the minimally-detailed global vegetation schemes in common use, both Burling et al. (2011) and this work measured EFs in temperate forest, and, more specifically, both studies measured EFs for prescribed fires burning in the understory of pine forests in the southeast US. However, there are some differences between the fires in our South Carolina (SC) study and the fires in North Carolina (NC) probed by Burling et al. (2011). The NC fuels were comprised mostly of fine woody material and foliage, whereas our SC study included at least three fires where the fuels were mostly litter. In addition, the NC fire emissions were measured after an exceptionally wet spring, while the SC fires were sampled in the fall after a prolonged drought. Multiple factors likely contributed to the differences between these two studies (Korontzi et al., 2003) and the effect of individual factors cannot be resolved from the available data. However, taken together, the two campaigns cover a more complete range of relevant environmental and fuel conditions and provide a much-improved picture of the mean and natural variability for EFs for prescribed fires within a fairly narrowly defined

**Table 3.** Ground-based and airborne emission factors (g kg<sup>-1</sup>) and MCE for all South Carolina burns studied in this work.

Fire Name	Ground-based					Airborne									
	Block 6 30 Oct 2011	Block 9b 1 Nov 2011	Block 22b 2 Nov 2011	Average Ground EF	±1σ	Block 6, RF01/02 30 Oct 2011	Block 9b, RF03/04 1 Nov 2011	Block 22b, RF05/06 2 Nov 2011	Pine Plantation, RF05 2 Nov 2011	Georgetown, RF07 7 Nov 2011	Francis Marion, RF08 8 Nov 2011	Bamberg, RF09 10 Nov 2011	Average Airborne EF	±1σ	
MCE	0.876	0.858	0.789	0.841	0.046	0.932	0.919	0.935	0.904	0.938	0.933	0.957	0.931	0.016	
FTIR Species <sup>a</sup>															
Carbon Dioxide (CO <sub>2</sub> )	1554	1496	1305	1452	130	1674	1643	1679	1606	1696	1686	1739	1675	42	
Carbon Monoxide (CO)	140	158	222	173	43	78	92	74	109	72	78	49	79	19	
Methane (CH <sub>4</sub> )	5.20	11.50	10.34	9.01	3.35	1.74	2.08	2.01	6.66	2.22	1.88	2.02	2.66	1.77	
Acetylene (C <sub>2</sub> H <sub>2</sub> )	0.25	0.22	0.14	0.20	0.06	0.35	0.24	0.20	0.28	0.73	0.43	0.45	0.38	0.18	
Ethylene (C <sub>2</sub> H <sub>4</sub> )	0.89	1.53	1.25	1.22	0.32	1.21	1.23	0.94	1.34	1.62	1.27	0.60	1.17	0.32	
Propylene (C <sub>3</sub> H <sub>6</sub> )	0.40	1.02	1.00	0.81	0.35	0.55	0.70	0.51	0.84	0.29	0.54	0.23	0.52	0.21	
Formaldehyde (HCHO)	1.79	2.42	2.51	2.24	0.39	1.87	2.11	1.70	1.98	2.13	1.97	1.36	1.87	0.27	
Methanol (CH <sub>3</sub> OH)	2.35	6.42	3.60	4.12	2.09	1.18	1.45	1.16	2.09	1.53	1.08	0.90	1.20	0.49	
Acetic Acid (CH <sub>3</sub> COOH)	1.03	3.84	2.42	2.43	1.41	1.24	0.75	1.25	1.85	2.33	1.60	2.82	1.69	0.71	
Phenol (C <sub>6</sub> H <sub>5</sub> OH)	0.11	0.18	0.16	0.15	0.04	0.23	0.21	0.12	0.53	bd <sup>b</sup>	bd <sup>b</sup>	bd <sup>b</sup>	0.27	0.18	
Furan (C <sub>4</sub> H <sub>4</sub> O)	0.44	1.60	0.86	0.97	0.59	0.20	0.20	0.11	0.54	bd <sup>b</sup>	bd <sup>b</sup>	bd <sup>b</sup>	0.27	0.19	
Hydrogen Cyanide (HCN)	0.95	0.85	1.12	0.98	0.14	0.74	0.82	0.84	1.58	0.94	0.68	0.42	0.66	0.27	
Ammonia (NH <sub>3</sub> )	0.05	0.23	0.33	0.20	0.15	0.11	0.13	0.14	0.13	bd <sup>b</sup>	bd <sup>b</sup>	bd <sup>b</sup>	0.11	0.03	
1,3-Butadiene (C <sub>4</sub> H <sub>6</sub> )	0.10	0.15	0.09	0.11	0.03	0.26	0.32	0.26	0.24	0.19	0.28	bd <sup>b</sup>	0.26	0.04	
Isoprene (C <sub>5</sub> H <sub>8</sub> ) <sup>c</sup>	0.08	0.02	0.15	0.08	0.06	0.18	0.14	0.14	0.11	–	–	–	0.14	0.03	
Limonene (C <sub>10</sub> H <sub>16</sub> )	2.58	bd <sup>b</sup>	5.36	3.97	1.97	1.62	2.84	1.65	0.09	bd <sup>b</sup>	1.20	bd <sup>b</sup>	1.48	0.99	
Formic Acid (HCOOH)	bd <sup>b</sup>	bd <sup>b</sup>	bd <sup>b</sup>	–	–	0.68	0.09	0.11	0.03	bd <sup>b</sup>	0.08	bd <sup>b</sup>	0.08	0.03	
Glycolaldehyde (C <sub>2</sub> H <sub>4</sub> O <sub>2</sub> )	bd <sup>b</sup>	bd <sup>b</sup>	bd <sup>b</sup>	–	–	0.41	0.10	0.31	0.60	0.69	0.24	bd <sup>b</sup>	0.39	0.22	
Nitrous Acid (HONO)	bd <sup>b</sup>	bd <sup>b</sup>	bd <sup>b</sup>	–	–	0.40	bd <sup>b</sup>	0.38	bd <sup>b</sup>	0.34	0.60	bd <sup>b</sup>	0.43	0.12	
Nitric Oxide (NO)	bd <sup>b</sup>	bd <sup>b</sup>	bd <sup>b</sup>	–	–	0.37	0.28	0.28	bd <sup>b</sup>	bd <sup>b</sup>	0.23	0.41	0.32	0.07	
Nitrogen Dioxide (NO <sub>2</sub> )	bd <sup>b</sup>	bd <sup>b</sup>	bd <sup>b</sup>	–	–	2.21	1.30	1.58	1.89	bd <sup>b</sup>	1.52	1.83	1.72	0.32	
Nitrogen Oxides (NO <sub>x</sub> as NO)	bd <sup>b</sup>	bd <sup>b</sup>	bd <sup>b</sup>	–	–	1.63	1.03	1.25	1.23	bd <sup>b</sup>	1.17	1.53	1.31	0.23	
WAS species															
Carbonyl Sulfide (OCS)	0.011	0.017	0.338	0.122	0.187	0.010	0.011	0.014	0.006	–	–	–	0.010	0.003	
Dimethyl Sulfide (DMS, C <sub>2</sub> H <sub>6</sub> S)	0.007	0.011	0.078	0.032	0.040	0.011	0.004	0.010	0.008	–	–	–	0.008	0.003	
Ethane (C <sub>2</sub> H <sub>6</sub> )	0.503	2.033	5.632	2.723	2.633	0.261	0.347	0.324	1.026	–	–	–	0.489	0.359	
Propyne (C <sub>3</sub> H <sub>4</sub> )	0.018	0.009	0.031	0.019	0.011	0.057	0.059	0.048	0.008	–	–	–	0.056	0.006	
1-Butyne (C <sub>4</sub> H <sub>6</sub> )	0.001	0.001	0.002	0.001	0.001	0.005	0.005	0.005	0.061	–	–	–	0.006	0.002	
2-Butyne (C <sub>4</sub> H <sub>6</sub> )	0.001	0.001	0.003	0.002	0.001	0.003	0.003	0.003	0.007	–	–	–	0.004	0.002	
1,2-Propadiene (C <sub>3</sub> H <sub>4</sub> )	0.005	0.002	0.008	0.005	0.003	0.016	0.015	0.013	0.017	–	–	–	0.015	0.002	
Propane (C <sub>3</sub> H <sub>8</sub> )	0.171	0.544	1.692	0.802	0.793	0.081	0.115	0.116	0.299	–	–	–	0.153	0.099	
<i>i</i> -Butane (C <sub>4</sub> H <sub>10</sub> )	0.012	0.026	0.169	0.069	0.087	0.007	0.007	0.011	0.016	–	–	–	0.010	0.005	
<i>n</i> -Butane (C <sub>4</sub> H <sub>10</sub> )	0.032	0.122	0.431	0.195	0.209	0.020	0.033	0.033	0.058	–	–	–	0.036	0.016	
1-Butene (C <sub>4</sub> H <sub>8</sub> )	0.066	0.200	0.478	0.248	0.210	0.105	0.118	0.122	0.182	–	–	–	0.131	0.034	
<i>i</i> -Butene (C <sub>4</sub> H <sub>8</sub> )	0.063	0.150	0.603	0.272	0.290	0.073	0.079	0.090	0.111	–	–	–	0.088	0.017	
<i>trans</i> -2-Butene (C <sub>4</sub> H <sub>8</sub> )	0.026	0.099	0.212	0.112	0.093	0.021	0.028	0.029	0.061	–	–	–	0.035	0.018	
<i>cis</i> -2-Butene (C <sub>4</sub> H <sub>8</sub> )	0.020	0.081	0.166	0.089	0.073	0.017	0.021	0.022	0.052	–	–	–	0.028	0.016	
<i>i</i> -Pentane (C <sub>5</sub> H <sub>12</sub> )	0.005	0.011	0.074	0.030	0.039	0.005	0.009	0.008	0.007	–	–	–	0.007	0.002	
<i>n</i> -Pentane (C <sub>5</sub> H <sub>12</sub> )	0.014	0.054	0.218	0.095	0.108	0.014	0.019	0.021	0.022	–	–	–	0.019	0.003	
1-Pentene (C <sub>5</sub> H <sub>10</sub> )	0.013	0.060	0.123	0.065	0.055	0.028	0.032	0.035	0.024	–	–	–	0.030	0.005	
<i>trans</i> -2-Pentene (C <sub>5</sub> H <sub>10</sub> )	0.009	0.034	0.078	0.040	0.035	0.011	0.012	0.013	0.026	–	–	–	0.016	0.007	
<i>cis</i> -2-Pentene (C <sub>5</sub> H <sub>10</sub> )	0.005	0.018	0.039	0.021	0.017	0.006	0.008	0.007	0.016	–	–	–	0.009	0.004	
3-Methyl-1-Butene (C <sub>5</sub> H <sub>10</sub> )	0.009	0.011	0.055	0.025	0.026	0.012	0.014	0.013	0.016	–	–	–	0.014	0.002	
2-Methyl-1-Butene (C <sub>5</sub> H <sub>10</sub> )	0.013	0.029	0.096	0.046	0.044	0.015	0.018	0.018	0.027	–	–	–	0.019	0.005	
Methyl Acetate (C <sub>3</sub> H <sub>6</sub> O <sub>2</sub> )	0.017	0.062	0.128	0.069	0.056	bd <sup>b</sup>	bd <sup>b</sup>	bd <sup>b</sup>	0.025	–	–	–	0.015	0.016	
2-Methyl-2-Butene (C <sub>5</sub> H <sub>10</sub> )	0.010	0.036	0.169	0.071	0.085	0.022	0.022	0.025	0.025	–	–	–	0.024	0.002	
1,3-Pentadiene (C <sub>5</sub> H <sub>8</sub> )	0.007	0.022	0.046	0.025	0.020	0.022	0.016	0.023	0.031	–	–	–	0.023	0.006	
1-Heptene (C <sub>7</sub> H <sub>14</sub> )	0.011	0.061	0.100	0.057	0.045	0.026	0.022	0.036	0.015	–	–	–	0.025	0.009	
1-Octene (C <sub>8</sub> H <sub>16</sub> )	0.012	0.064	0.122	0.066	0.055	0.021	0.022	0.026	0.018	–	–	–	0.022	0.003	
Cyclopentene (C <sub>5</sub> H <sub>8</sub> )	0.021	0.043	0.145	0.070	0.066	0.043	0.043	0.051	0.042	–	–	–	0.045	0.004	
<i>n</i> -Hexane (C <sub>6</sub> H <sub>14</sub> )	0.010	0.046	0.128	0.062	0.060	0.008	0.015	0.013	0.012	–	–	–	0.012	0.003	
<i>n</i> -Heptane (C <sub>7</sub> H <sub>16</sub> )	0.005	0.042	0.082	0.043	0.039	0.006	0.015	0.009	0.005	–	–	–	0.008	0.005	
<i>n</i> -Octane (C <sub>8</sub> H <sub>18</sub> )	0.004	0.032	0.071	0.036	0.034	0.004	0.022	0.006	0.000	–	–	–	0.008	0.010	
Nonane (C <sub>9</sub> H <sub>20</sub> )	0.004	0.025	0.073	0.034	0.035	0.003	0.063	0.008	bd <sup>b</sup>	–	–	–	0.025	0.033	
<i>n</i> -Decane (C <sub>10</sub> H <sub>22</sub> )	0.007	0.021	0.053	0.027	0.024	bd <sup>b</sup>	0.077	bd <sup>b</sup>	bd <sup>b</sup>	–	–	–	0.077	–	
2,3-Dimethylbutane (C <sub>6</sub> H <sub>14</sub> )	0.001	0.002	0.011	0.005	0.005	bd <sup>b</sup>	bd <sup>b</sup>	bd <sup>b</sup>	bd <sup>b</sup>	–	–	–	–	–	
2-Methylpentane (C <sub>6</sub> H <sub>14</sub> )	0.006	0.010	0.071	0.029	0.036	0.004	0.010	0.006	0.006	–	–	–	0.007	0.002	
3-Methylpentane (C <sub>6</sub> H <sub>14</sub> )	0.001	0.003	0.012	0.005	0.006	0.002	0.005	0.002	0.003	–	–	–	0.003	0.001	
Benzene (C <sub>6</sub> H <sub>6</sub> )	0.268	0.429	1.712	0.803	0.791	0.251	0.254	0.284	0.345	–	–	–	0.283	0.043	
Toluene (C <sub>6</sub> H <sub>5</sub> CH <sub>3</sub> )	0.515	0.283	0.938	0.579	0.332	0.164	0.204	0.190	0.237	–	–	–	0.199	0.031	
Ethylbenzene (C <sub>8</sub> H <sub>10</sub> )	0.064	0.039	0.112	0.072	0.037	0.035	0.061	0.026	0.032	–	–	–	0.039	0.016	
<i>p</i> -Xylene (C <sub>8</sub> H <sub>10</sub> )	0.017	0.034	0.092	0.048	0.039	0.027	0.050	0.022	0.024	–	–	–	0.031	0.013	
<i>m</i> -Xylene (C <sub>8</sub> H <sub>10</sub> )	0.112	0.074	0.555	0.247	0.267	0.054	0.009	0.070	0.062	–	–	–	0.049	0.027	
<i>o</i> -Xylene (C <sub>8</sub> H <sub>10</sub> )	0.026	0.043	0.146	0.071	0.065	0.021	0.042	0.022	0.016	–	–	–	0.025	0.011	
Styrene (C <sub>8</sub> H <sub>8</sub> )	0.059	0.031	0.101	0.064	0.035	0.043	0.035	0.042	0.040	–	–	–	0.040	0.003	
<i>i</i> -Propylbenzene (C <sub>9</sub> H <sub>12</sub> )	0.006	0.013	bd <sup>b</sup>	0.009	0.005	bd <sup>b</sup>	bd <sup>b</sup>	bd <sup>b</sup>	0.002	–	–	–	0.002	–	
<i>n</i> -Propylbenzene (C <sub>9</sub> H <sub>12</sub> )	0.012	0.010	0.072	0.031	0.035	0.004	0.008	0.004	0.003	–	–	–	0.005	0.002	
3-Ethyltoluene (C <sub>9</sub> H <sub>12</sub> )	0.157	0.016	0.293	0.155	0.139	0.028	0.046	0.023	0.018	–					

**Table 4.** Statistics for the linear regression of EF as a function of MCE for combined ground-based and airborne fire-average measurements. Values in parentheses represent 1- $\sigma$  standard deviation.

FTIR Species	Slope	Y-Intercept	R <sup>2</sup>	# Samples
Methane (CH <sub>4</sub> )	-65.01 (12.65)	63.34 (11.45)	0.77	10
Acetylene (C <sub>2</sub> H <sub>2</sub> )	2.07 (0.96)	-1.54 (0.87)	0.37	10
Ethylene (C <sub>2</sub> H <sub>4</sub> )	-1.50 (2.06)	2.55 (1.87)	0.06	10
Propylene (C <sub>3</sub> H <sub>6</sub> )	-4.12 (1.28)	4.34 (1.16)	0.57	10
Formaldehyde (HCHO)	-4.97 (1.58)	6.48 (1.43)	0.55	10
Methanol (CH <sub>3</sub> OH)	-25.72 (8.39)	25.33 (7.60)	0.54	10
Acetic Acid (CH <sub>3</sub> COOH)	-5.49 (6.36)	6.88 (5.76)	0.09	10
Phenol (C <sub>6</sub> H <sub>5</sub> OH)	0.53 (1.20)	-0.26 (1.07)	0.04	7
Furan (C <sub>4</sub> H <sub>4</sub> O)	-6.65 (3.40)	6.47 (3.02)	0.43	7
Hydrogen Cyanide (HCN)	-2.75 (1.67)	3.24 (1.51)	0.25	10
Ammonia (NH <sub>3</sub> )	-1.48 (0.45)	1.47 (0.41)	0.64	8
1,3-Butadiene (C <sub>4</sub> H <sub>6</sub> )	1.32 (0.38)	-0.97 (0.35)	0.63	9
Isoprene (C <sub>5</sub> H <sub>8</sub> )	0.26 (0.43)	-0.11 (0.38)	0.07	7
Limonene (C <sub>10</sub> H <sub>16</sub> )	-25.8 (8.23)	25.3 (7.41)	0.66	7
Formic Acid (HCOOH)	-1.78 (0.67)	-1.57 (0.62)	0.70	5
Glycolaldehyde (C <sub>2</sub> H <sub>4</sub> O <sub>2</sub> )	-0.84 (8.63)	1.17 (8.00)	0.00	6
Nitrous Acid (HONO)	-25.7 (25.7)	24.5 (24.0)	0.33	4
Nitric Oxide (NO)	3.56 (2.31)	-3.02 (2.16)	0.44	5
Nitrogen Dioxide (NO <sub>2</sub> )	1.90 (9.02)	-0.05 (8.39)	0.01	6
Nitrogen Oxides (NO <sub>x</sub> as NO)	6.99 (5.42)	-5.19 (5.04)	0.29	6
WAS species				
Carbonyl Sulfide (OCS)	-2.00 (0.57)	1.83 (0.51)	0.71	7
Dimethyl Sulfide (DMS, C <sub>2</sub> H <sub>6</sub> S)	-0.43 (0.12)	0.40 (0.11)	0.70	7
Ethane (C <sub>2</sub> H <sub>6</sub> )	-34.95 (6.09)	32.47 (5.42)	0.87	7
Propyne (C <sub>3</sub> H <sub>4</sub> )	0.25 (0.14)	-0.18 (0.13)	0.39	7
1-Butyne (C <sub>4</sub> H <sub>6</sub> )	0.032 (0.017)	-0.025 (0.015)	0.42	7
2-Butyne (C <sub>4</sub> H <sub>6</sub> )	0.012 (0.016)	-0.007 (0.014)	0.09	7
1,2-Propadiene (C <sub>3</sub> H <sub>4</sub> )	0.071 (0.038)	-0.052 (0.034)	0.41	7
Propane (C <sub>3</sub> H <sub>8</sub> )	-10.32 (1.784)	9.59 (1.67)	0.86	7
<i>i</i> -Butane (C <sub>4</sub> H <sub>10</sub> )	-1.00 (0.24)	0.93 (0.22)	0.78	7
<i>n</i> -Butane (C <sub>4</sub> H <sub>10</sub> )	-2.59 (0.53)	2.40 (0.47)	0.83	7
1-Butene (C <sub>4</sub> H <sub>8</sub> )	-2.26 (0.63)	2.19 (0.56)	0.72	7
<i>i</i> -Butene (C <sub>4</sub> H <sub>8</sub> )	-3.26 (0.82)	3.06 (0.73)	0.76	7
<i>trans</i> -2-Butene (C <sub>4</sub> H <sub>8</sub> )	-1.23 (0.23)	1.16 (0.21)	0.85	7
<i>cis</i> -2-Butene (C <sub>4</sub> H <sub>8</sub> )	-0.97 (0.18)	0.91 (0.16)	0.85	7
<i>i</i> -Pentane (C <sub>5</sub> H <sub>12</sub> )	-0.42 (0.12)	0.39 (0.10)	0.72	7
<i>n</i> -Pentane (C <sub>5</sub> H <sub>12</sub> )	1.28 (0.30)	1.18 (0.26)	0.79	7
1-Pentene (C <sub>5</sub> H <sub>10</sub> )	-0.60 (0.17)	0.58 (0.15)	0.71	7
<i>trans</i> -2-Pentene (C <sub>5</sub> H <sub>10</sub> )	-0.43 (0.09)	0.40 (0.08)	0.80	7
<i>cis</i> -2-Pentene (C <sub>5</sub> H <sub>10</sub> )	-0.20 (0.05)	0.19 (0.04)	0.78	7
3-Methyl-1-Butene (C <sub>5</sub> H <sub>10</sub> )	-0.248 (0.085)	0.238 (0.076)	0.63	7
2-Methyl-1-Butene (C <sub>5</sub> H <sub>10</sub> )	-0.49 (0.12)	0.47 (0.11)	0.76	7
Methyl Acetate (C <sub>3</sub> H <sub>6</sub> O <sub>2</sub> )	-0.87 (0.16)	0.80 (0.14)	0.90	5
2-Methyl-2-Butene (C <sub>5</sub> H <sub>10</sub> )	-0.90 (0.26)	0.84 (0.23)	0.70	7
1,3-Pentadiene (C <sub>5</sub> H <sub>8</sub> )	-0.14 (0.09)	0.15 (0.08)	0.34	7
1-Heptene (C <sub>7</sub> H <sub>14</sub> )	-0.49 (0.16)	0.47 (0.14)	0.65	7
1-Octene (C <sub>8</sub> H <sub>16</sub> )	-0.67 (0.16)	0.64 (0.14)	0.78	7
Cyclopentene (C <sub>5</sub> H <sub>8</sub> )	-0.58 (0.23)	0.57 (0.21)	0.55	7
<i>n</i> -Hexane (C <sub>6</sub> H <sub>14</sub> )	-0.77 (0.16)	0.72 (0.14)	0.83	7
<i>n</i> -Heptane (C <sub>7</sub> H <sub>16</sub> )	-0.50 (0.11)	0.47 (0.10)	0.81	7
<i>n</i> -Octane (C <sub>8</sub> H <sub>18</sub> )	-0.42 (0.11)	0.39 (0.10)	0.75	7
Nonane (C <sub>9</sub> H <sub>20</sub> )	-0.32 (0.22)	0.31 (0.20)	0.34	6
<i>n</i> -Decane (C <sub>10</sub> H <sub>22</sub> )	0.09 (0.41)	-0.04 (0.35)	0.02	4
2,3-Dimethylbutane (C <sub>6</sub> H <sub>14</sub> )	-0.12 (0.01)	0.10 (0.01)	0.99	3
2-Methylpentane (C <sub>6</sub> H <sub>14</sub> )	-0.40 (0.11)	0.37 (0.10)	0.74	7
3-Methylpentane (C <sub>6</sub> H <sub>14</sub> )	-0.055 (0.020)	0.053 (0.018)	0.59	7
Benzene (C <sub>6</sub> H <sub>6</sub> )	-9.03 (2.22)	8.52 (1.98)	0.77	7
Toluene (C <sub>6</sub> H <sub>5</sub> CH <sub>3</sub> )	-4.95 (0.96)	4.75 (0.85)	0.84	7
Ethylbenzene (C <sub>8</sub> H <sub>10</sub> )	-0.48 (0.15)	0.47 (0.13)	0.68	7
<i>p</i> -Xylene (C <sub>8</sub> H <sub>10</sub> )	-0.38 (0.15)	0.37 (0.13)	0.56	7
<i>m</i> -Xylene (C <sub>8</sub> H <sub>10</sub> )	-3.16 (0.79)	2.93 (0.70)	0.76	7
<i>o</i> -Xylene (C <sub>8</sub> H <sub>10</sub> )	-0.76 (0.19)	0.72 (0.17)	0.76	7
Styrene (C <sub>8</sub> H <sub>8</sub> )	-0.36 (0.13)	0.37 (0.11)	0.62	7
<i>i</i> -Propylbenzene (C <sub>9</sub> H <sub>12</sub> )	-1.23 (0.07)	0.21 (0.06)	0.92	3
<i>n</i> -Propylbenzene (C <sub>9</sub> H <sub>12</sub> )	-0.42 (0.10)	0.39 (0.09)	0.78	7
3-Ethyltoluene (C <sub>9</sub> H <sub>12</sub> )	-1.67 (0.51)	1.57 (0.45)	0.68	7
4-Ethyltoluene (C <sub>9</sub> H <sub>12</sub> )	-0.73 (0.32)	0.69 (0.29)	0.50	7
2-Ethyltoluene (C <sub>9</sub> H <sub>12</sub> )	-0.10 (0.05)	0.10 (0.05)	0.41	7
1,3,5-Trimethylbenzene (C <sub>9</sub> H <sub>12</sub> )	-0.11 (0.15)	0.12 (0.13)	0.12	6
1,2,4-Trimethylbenzene (C <sub>9</sub> H <sub>12</sub> )	-1.20 (0.50)	1.16 (0.45)	0.53	7
1,2,3-Trimethylbenzene (C <sub>9</sub> H <sub>12</sub> )	-2.26 (0.77)	2.11 (0.69)	0.63	7
<i>p</i> -Cymene (C <sub>10</sub> H <sub>14</sub> )	-8.34 (0.44)	7.57 (0.38)	1.00	3
$\alpha$ -Pinene (C <sub>10</sub> H <sub>16</sub> )	-38.49 (9.92)	35.35 (8.82)	0.75	7
$\beta$ -Pinene (C <sub>10</sub> H <sub>16</sub> )	-3.84 (0.88)	3.57 (0.78)	0.79	7
4-Carene (C <sub>10</sub> H <sub>16</sub> )	-1.22 (0.18)	1.14 (0.16)	0.92	6

**Table 4.** Continued.

WAS species	Slope	Y-Intercept	R <sup>2</sup>	# Samples
Camphene (C <sub>10</sub> H <sub>16</sub> )	-4.78 (1.36)	4.46 (1.19)	0.86	4
Myrcene (C <sub>10</sub> H <sub>16</sub> )	-0.74 (0.34)	0.69 (0.29)	0.83	3
Acetonitrile (CH <sub>3</sub> CN)	-7.64 (3.41)	6.92 (2.95)	0.72	4
Acrylonitrile (C <sub>3</sub> H <sub>3</sub> N)	0.15 (0.22)	-0.09 (0.19)	0.09	7
2-Methylfuran (C <sub>5</sub> H <sub>6</sub> O)	-7.55 (1.24)	7.06 (1.10)	0.88	7
2-Ethylfuran (C <sub>6</sub> H <sub>8</sub> O)	-0.43 (0.08)	0.40 (0.07)	0.86	7
2,5-Dimethylfuran (C <sub>6</sub> H <sub>8</sub> O)	-2.53 (0.47)	2.35 (0.42)	0.85	7
Acetaldehyde (CH <sub>3</sub> CHO)	-15.52 (4.11)	14.80 (3.65)	0.74	7
<i>n</i> -Butanal (C <sub>4</sub> H <sub>8</sub> O)	-0.37 (0.15)	0.37 (0.14)	0.54	7
2-Methylpropanal (C <sub>4</sub> H <sub>8</sub> O)	-1.65 (0.47)	1.52 (0.41)	0.71	7
3-Methylbutanal (C <sub>5</sub> H <sub>10</sub> O)	-1.77 (0.46)	1.64 (0.41)	0.75	7
Acrolein (C <sub>3</sub> H <sub>4</sub> O)	-3.91 (1.65)	3.86 (1.46)	0.53	7
Methacrolein (C <sub>4</sub> H <sub>6</sub> O)	-0.80 (0.25)	0.77 (0.22)	0.67	7
2-Furaldehyde (C <sub>5</sub> H <sub>4</sub> O <sub>2</sub> )	-0.36 (0.47)	0.39 (0.42)	0.10	7
Acetone (C <sub>3</sub> H <sub>6</sub> O)	-16.26 (4.34)	15.46 (3.86)	0.74	7
Methyl ethyl ketone (C <sub>4</sub> H <sub>8</sub> O)	-3.39 (0.64)	3.21 (0.57)	0.85	7
Methyl vinyl ketone (C <sub>4</sub> H <sub>6</sub> O)	-2.06 (0.49)	1.94 (0.44)	0.78	7
3-Methyl-2-Butanone (C <sub>5</sub> H <sub>10</sub> O)	-0.76 (0.13)	0.71 (0.12)	0.86	7
3-Methyl-3-buten-2-one (C <sub>5</sub> H <sub>8</sub> O)	-3.10 (0.60)	2.87 (0.53)	0.84	7
Ethanol (CH <sub>3</sub> CH <sub>2</sub> OH)	-0.11 (0.08)	0.12 (0.07)	0.34	6
Nitromethane (CH <sub>3</sub> NO <sub>2</sub> )	0.16 (0.39)	-0.04 (0.35)	0.03	7

ecosystem classification. Our SC study-average MCE from airborne sampling was  $0.931 \pm 0.016$ , which is almost within 1- $\sigma$  standard deviation of the average airborne MCE for the NC conifer forest understory burns ( $0.948 \pm 0.006$ ). Of the 17 species (besides CO<sub>2</sub> and CO) measured from the aircraft in both studies, only six compounds have EFs that agree within 35 %. We observed 52 % lower NO<sub>x</sub> in SC, along with 22 and 33 % lower EF(HONO) and EF(NH<sub>3</sub>), respectively (Fig. 6a). The fuels burned in the NC fires likely included more foliage, which typically has a high N content compared to litter (Susott et al., 1996). In contrast to the N-containing species, airborne EFs for all non-methane hydrocarbons (NMHCs) and oxygenated volatile organic compounds (OVOCs) were much higher in SC.

We can also compare the ground-based measurements from the two studies. Ground-based sampling of SC fires resulted in an MCE of  $0.841 \pm 0.046$ , very similar to the  $0.838 \pm 0.055$  MCE measured in NC. EF(CO) and EF(CO<sub>2</sub>) agreed within 4 %, and EF(CH<sub>4</sub>) agreed within 30 %. However, large differences were observed for most of the other 11 compounds measured in both studies. We report 73–97 % lower EFs in SC for all NMHCs that were measured in both studies (C<sub>2</sub>H<sub>2</sub>, C<sub>2</sub>H<sub>4</sub>, C<sub>3</sub>H<sub>6</sub>, 1,3-butadiene, and isoprene), which is the opposite of the EF(NMHC) comparison for the airborne measurements. We also observe 13–78 % higher EFs in the SC ground-based samples for all the OVOCs measured in both studies (HCHO, CH<sub>3</sub>OH, CH<sub>3</sub>COOH, and C<sub>4</sub>H<sub>4</sub>O), which mimics the airborne comparison (Fig. 6b). The ground-based EF(NMHC) from SC, despite being lower than the ground-based EF(NMHC) in NC, are higher than all EF(NMHC) measured in laboratory burns of southeast pine litter (Burling et al., 2010). However, the MCE for the laboratory litter fires ( $0.894 \pm 0.017$ ) was higher than both the NC and SC ground-based MCEs. This brief overview makes it clear that large differences can be observed even in

**Table 5.** Airborne and ground-based molar emission ratios to CO of measured terpenes from SC fires, shown in order of abundance.

Fire Name	Airborne								Average Airborne ER	±1σ
	Block 6	Block 9b	Block 22b	Pine Plantation	Georgetown	Francis Marion	Bamberg			
Date	30 Oct 2011	1 Nov 2011	2 Nov 2011	2 Nov 2011	7 Nov 2011	8 Nov 2011	10 Nov 2011			
Limonene	4.30E-03	6.38E-03	4.60E-03	1.78E-04	bdl*	3.19E-03	bdl	3.73E-03	2.29E-03	
Isoprene	9.44E-04	6.20E-04	7.83E-04	3.96E-04	–	–	–	6.86E-04	2.34E-04	
α-Pinene	2.27E-04	2.30E-04	1.92E-04	2.20E-04	–	–	–	2.17E-04	1.73E-05	
β-Pinene	1.63E-04	1.37E-04	1.44E-04	6.14E-05	–	–	–	1.26E-04	4.47E-05	
Camphene	6.05E-05	bdl	bdl	1.26E-05	–	–	–	3.66E-05	3.39E-05	
4-Carene	3.68E-05	2.32E-05	1.56E-05	1.51E-05	–	–	–	2.27E-05	1.01E-05	
Myrcene	bdl	bdl	bdl	1.46E-05	–	–	–	1.46E-05	–	
ΣMonoterpenes	4.79E-03	6.77E-03	4.95E-03	5.01E-04	–	3.19E-03	–	4.04E-03	2.35E-03	
ΣTerpenes	5.73E-03	7.39E-03	5.73E-03	8.97E-04	–	3.19E-03	–	4.59E-03	2.55E-03	
ΣNMOC	1.14E-01	1.02E-01	1.20E-01	1.02E-01	1.05E-01	8.85E-02	1.02E-01	1.05E-01	9.94E-03	

Fire Name	Ground-based				
	Block 6	Block 9b	Block 22b	Average Ground ER	±1σ
Date	30 Oct 2011	1 Nov 2011	2 Nov 2011		
Limonene	3.78E-03	bdl	4.97E-03	4.37E-03	8.41E-04
α-Pinene	2.46E-03	3.37E-05	5.78E-03	2.76E-03	2.89E-03
Camphene	6.26E-04	bdl	6.09E-04	6.18E-04	1.25E-05
β-Pinene	2.93E-04	1.19E-04	6.09E-04	3.40E-04	2.48E-04
Isoprene	2.23E-04	6.52E-05	2.79E-04	1.89E-04	1.11E-04
4-Carene	1.47E-04	bdl	1.61E-04	1.54E-04	9.83E-06
Myrcene	9.89E-05	bdl	9.68E-05	9.78E-05	1.48E-06
ΣMonoterpenes	7.40E-03	1.52E-04	1.22E-02	6.59E-03	6.08E-03
ΣTerpenes	7.62E-03	2.18E-04	1.25E-02	6.78E-03	6.19E-03
ΣNMOC	7.17E-02	1.20E-01	1.32E-01	1.08E-01	3.19E-02

\* bdl = below detection limit.

study-average emission factors for nominally similar ecosystems, most likely due in part to inherent large variability in the natural environment: weather, fuels, etc.

### 3.3 Observation of large initial emissions of terpenes

#### 3.3.1 Background levels and production in smoke plumes

Terpenes-hemiterpenes (isoprene), monoterpenes (C<sub>10</sub>H<sub>16</sub>), and sesquiterpenes (C<sub>15</sub>H<sub>24</sub>) – are emitted by plants in response to injury, disease, and other reasons (Paine et al., 1987; Guenther et al., 2006). Isoprene is synthesized by plants and then immediately emitted, but it is also a combustion product that is, for instance, emitted in high quantities by smoldering peat (Christian et al., 2003). In contrast, monoterpenes can be stored for months in plant tissue. A fraction of the synthesized monoterpenes are emitted immediately following synthesis, but the highest concentration of these compounds immediately adjacent to the plant is only a few ppb under normal conditions (Bouvier-Brown et al., 2009). However, very large concentrations of monoterpenes may be emitted into the gas phase (or “boiled off” via distillation) due to exposure to heat from fires (Simpson et al., 2011). Thus, the absolute mixing ratios of terpenes in relatively undiluted fire emissions can exceed several ppmv and

are much greater than the mixing ratios of these compounds from natural vegetative emissions.

#### 3.3.2 High levels of terpenes in fresh smoke

The initial emissions of terpenes from biomass burning have been measured several times previously. Isoprene EF have been measured for some biomass fuels (Christian et al., 2003; Yokelson et al., 2007; Akagi et al., 2011; Simpson et al., 2011). Additionally, Yokelson et al. (1996) and Burling et al. (2011) noted large, IR spectral features in smoke similar to monoterpene absorption, suggesting possible large emissions of monoterpenes. Simpson et al. (2011) reported large EFs for two monoterpenes, α-pinene and β-pinene, as measured by WAS from Canadian boreal forest fires during the Arctic Research of the Composition of the Troposphere from Aircraft and Satellites (ARCTAS) campaign. In this work we present the first quantitative FTIR observations of a monoterpene (limonene) in smoke along with an expanded suite of monoterpenes measured by WAS including α-pinene, β-pinene, limonene, camphene, 4-carene, and myrcene – some for the first time from field fires. Our measured fire-averaged ERs of these monoterpenes (and isoprene) from the ground-based and airborne platforms are shown in order of abundance in Table 5. In the SC smoke plumes, limonene and α-pinene are the most abundant monoterpenes measured from

both the airborne and ground-based platforms, with limonene mixing ratios observed as high as 8.4 ppm.

Our study-averaged ER( $\Delta\alpha$ -pinene/ $\Delta$ CO) was more than 12 times higher in our ground-based measurements than in our airborne measurements (the Block 9b fire was an exception, where ER( $\Delta\alpha$ -pinene/ $\Delta$ CO) on the ground was  $\sim 7$  times lower than airborne). In contrast, the study-average ER( $\Delta$ limonene/ $\Delta$ CO) was only lower by a factor of 1.2 in the air (Table 5). The  $\alpha$ -pinene rate constants with respect to OH, O<sub>3</sub>, and NO<sub>3</sub> are slower than those of limonene with these oxidants, suggesting that the much lower  $\alpha$ -pinene/limonene ratio in lofted smoke that reached the aircraft is not due to atmospheric oxidation. We suggest that  $\alpha$ -pinene may be preferentially released from fuels that burn largely by RSC (duff, dead-down woody fuels, etc.) and thus is relatively more abundant in smoke that was poorly lofted in this study. The  $\Delta$ isoprene/ $\Delta$ CO ER was  $\sim 3.6$  times greater in the lofted emissions sampled from the air, suggesting that RSC fuels may produce lower isoprene to CO ratios than the fuels that typically produce the bulk of lofted smoke (fine fuels, Akagi et al., 2011).

Figure 7 shows EFs (g kg<sup>-1</sup>) of monoterpenes and isoprene measured in this work. In light of the platform-specific tendencies noted above, it is of interest to further compare our terpene EFs with the  $\alpha$ -pinene,  $\beta$ -pinene and isoprene EFs for boreal forest fires in Alberta, Canada measured by Simpson et al. (2011). Simpson et al. (2011) did not include limonene or other monoterpenes in their analysis due to the long analytical run-times required for the additional compounds. The sum of study-averaged  $\alpha$ - and  $\beta$ -pinene EFs from this work was  $2.97 \pm 3.24$  g kg<sup>-1</sup> and  $0.146 \pm 0.249$  g kg<sup>-1</sup> for the ground-based and airborne measurements, respectively. In comparison, the sum of  $\alpha$ - and  $\beta$ -pinene EFs obtained during the airborne study of Simpson et al. (2011) had an intermediate value of  $1.53 \pm 0.13$  g kg<sup>-1</sup> and was obtained at an intermediate MCE of 0.90. Boreal forests often have a much greater loading of dead-down woody fuels (due in part to slower decomposition) than temperate forests, and so relatively more of the emissions from these fuels may have been entrained in the lofted emissions sampled by Simpson et al. (2011). A higher contribution from the dead/down woody fuels would also be consistent with lower isoprene EFs of Simpson et al. (2011) ( $0.074 \pm 0.017$ ; Fig. 7). It should not be assumed, however, that unlofted smoke will always have lower abundance of isoprene than lofted smoke since a very high isoprene EF was observed by Christian et al. (2003) for smoldering peat. Finally, given that large EFs were observed for both  $\alpha$ - and  $\beta$ -pinene in the ARCTAS campaign, it is likely that high levels of additional terpenes were also present in the ARCTAS samples that were not measured.

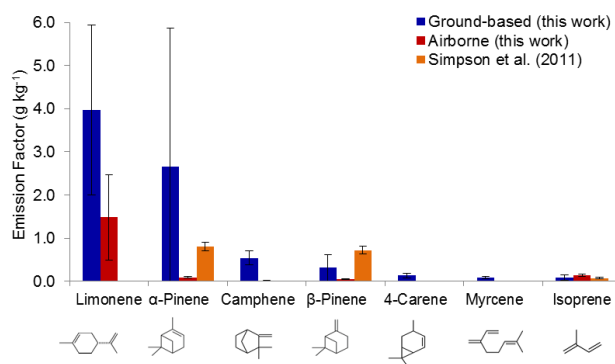


**Fig. 7.** Emission factors (g kg<sup>-1</sup>) of monoterpenes and isoprene measured in this work from ground-based (blue) and airborne (red) platforms. Molecular structures are shown below each compound. We compare with data from Simpson et al. (2011) who measured  $\alpha$ -pinene,  $\beta$ -pinene and isoprene only from an airborne platform (orange). Error bars represent the 1- $\sigma$  standard deviation in EF.

### 3.3.3 The influence of terpenes on smoke plume chemistry

We first assess the role of the dominant terpenes in daytime downwind VOC production in our biomass burning plumes. One important potential daytime oxidant – O<sub>3</sub> – was depleted in the freshest smoke via rapid reaction of background O<sub>3</sub> ( $\sim 50$ – $80$  ppb) with NO emitted by the fire (see Sect. 3.7 of this work; Yokelson et al., 2003b; Akagi et al., 2011, 2012). Thus, the reaction of limonene with OH would initially be the main daytime oxidation pathway forming low molecular weight products including methanol, formaldehyde, and acetone (Muller et al., 2005; Holzinger et al., 2005).  $\alpha$ -Pinene, the second most abundant monoterpene measured, reacts with OH to ultimately produce low molecular weight products such as acetone, formaldehyde, formic acid, and acetic acid (Capouet et al., 2004). Oxidation of terpenes via OH will be the main oxidation pathway for terpenes until O<sub>3</sub> levels rebound in the plume, which can happen in as little as 0.5 h, at which time oxidation by both O<sub>3</sub> and OH become important reaction channels for the remaining terpenes. For limonene and  $\alpha$ -pinene, we can estimate how long these species would remain in the plume given the elevated OH concentrations often found in biomass burning plumes ( $5 \times 10^6$  to  $1 \times 10^7$  molec cm<sup>-3</sup>, Hobbs et al., 2003; Yokelson et al., 2009; Akagi et al., 2012). Assuming a pseudo first-order decay of limonene and  $\alpha$ -pinene with respect to OH ( $k_{\text{OH}+\text{limonene}} = 1.7 \times 10^{-10}$  cm<sup>3</sup> molec<sup>-1</sup> s<sup>-1</sup>,  $k_{\text{OH}+\alpha\text{-pinene}} = 5.3 \times 10^{-11}$  cm<sup>3</sup> molec<sup>-1</sup> s<sup>-1</sup>; Bouvier-Brown et al., 2009) we estimate that 99% of limonene and  $\alpha$ -pinene will have reacted within 0.8–1.6 h and 2.5–4.9 h following emission, respectively, with the higher [OH] estimate corresponding to faster monoterpene loss. As discussed later in Sect. 3.7, O<sub>3</sub> can rebound to 80–100 ppb in as little as 1 h following emission (e.g. O<sub>3</sub>

levels can be well above background despite dilution of the plume). This suggests that there will typically be some unreacted limonene and  $\alpha$ -pinene remaining in the plume once O<sub>3</sub> recovers to significant levels. At an estimated O<sub>3</sub> mixing ratio of 80–100 ppb 1 h after emission, 19–32 % and 9–16 % of the remaining limonene and  $\alpha$ -pinene, respectively, would be due to oxidation via the O<sub>3</sub> channel ( $k_{\text{O}_3+\text{limonene}} = 2.0 \times 10^{-16} \text{ cm}^3 \text{ molec}^{-1} \text{ s}^{-1}$ ,  $k_{\text{O}_3+\alpha\text{-pinene}} = 8.4 \times 10^{-17} \text{ cm}^3 \text{ molec}^{-1} \text{ s}^{-1}$ ; Bouvier-Brown et al., 2009), making reaction with O<sub>3</sub> (and its byproducts) important though likely secondary to the OH reaction. Limonene reaction with O<sub>3</sub> has been shown to produce secondary photoproducts such as formic and acetic acid, acetaldehyde, methanol, formaldehyde, and acetone (Lee et al., 2006; Walser et al., 2007; Pan et al., 2009) dependent on limonene and ozone levels. Recent work suggests the oxidation of  $\alpha$ -pinene with O<sub>3</sub> produces low molecular weight byproducts including formaldehyde, acetaldehyde, formic acid, acetone, and acetic acid (Lee et al., 2006). Monoterpene ozonolysis also produces OH, with OH molar yields of 0.86, 0.7–0.85, and 1.15 for limonene,  $\alpha$ -pinene, and myrcene, respectively (Finlayson-Pitts and Pitts, 2000). Thus, reaction via the O<sub>3</sub> channel would generate OH, increasing the oxidative capacity of the plume and encouraging further plume evolution. High levels of OH lead to increased O<sub>3</sub> formation which may help explain the high O<sub>3</sub> formation rates observed during this campaign (Sect. 3.7). The small molecule oxidation products of the other monoterpenes measured in this work (such as  $\beta$ -pinene and myrcene) following oxidation by OH and O<sub>3</sub> are similar to those products already listed and include formaldehyde, formic and acetic acid, acetaldehyde, and acetone (Lee et al., 2006). Evidence of downwind growth in several of these VOCs has been previously observed in biomass burning plumes (Jost et al., 2003; Holzinger et al., 2005; Karl et al., 2007; Akagi et al., 2011). While much effort has gone into understanding and identifying monoterpene products, there is still considerable carbon mass tied up in unidentified species (Lee et al., 2006). In summary, since both the oxidant levels and the initial emissions of terpenes are highly variable in biomass burning plumes, we expect this to contribute to high variability in post-emission VOC production as discussed in Sect. 3.7 and more generally in Akagi et al. (2011).

We also briefly explore the oxidation products of terpenes at night when reaction via ozone and NO<sub>3</sub> becomes more favorable. In a small minority of prescribed fires and more commonly in wildfires (especially in the boreal forest), a large amount of fuel can be consumed at night by smoldering combustion (Turetsky et al., 2011). On occasion, flaming combustion can occur at night that is perhaps promoted by nighttime frontal passage (Vermote et al., 2009). In this circumstance, some of the NO<sub>x</sub> may be tied up as NO<sub>3</sub> (Tereszczuk et al., 2011) promoting the reactions of terpenes and NO<sub>3</sub>, which produce formaldehyde, nitric acid (HNO<sub>3</sub>),

and large organic nitrates and aldehydes, where the latter two products have oxidation products that are not well studied (Fry et al., 2011). Assuming generic O<sub>3</sub> and NO<sub>3</sub> nighttime mixing ratios of 35 ppb and 5 ppt, respectively (Finlayson-Pitts and Pitts, 2000; Vrekoussis et al., 2004), about 90 % of the monoterpenes in smoke would react with NO<sub>3</sub> and the remainder mostly with O<sub>3</sub>. Production of alkyl nitrates from NO<sub>3</sub> oxidation of fire-generated monoterpenes may tie up NO<sub>x</sub> for long-distance transport and may also change the composition of secondary aerosol. In summary, most prescribed fires burn mostly during the day and most of the terpenes generated will be oxidized by OH. However, some fires produce smoke at night. Nighttime combustion is usually dominated by smoldering combustion due to higher relative humidity, lower temperature, lighter surface winds, and other factors. Thus, nighttime smoke probably has low average MCE and high monoterpene content. Most of the monoterpenes emitted during the night would be oxidized by NO<sub>3</sub>.

Considerable work has been done to investigate SOA yields from monoterpene oxidation (Griffin et al., 1999; Spittler et al., 2006; Saathoff et al., 2009; Fry et al., 2011). While SOA formation via nucleation processes has been observed, the more common path for SOA formation occurs via condensation of gas-phase oxidation products onto pre-existing aerosol, given the ubiquitous presence of condensation surfaces in the atmosphere (Hamilton et al., 2011). Limonene, the dominant monoterpene, is especially susceptible to oxidation with two C=C double bonds (a.k.a. reactive sites, Fig. 7), providing a quick, direct route to forming low-vapor pressure oxidation products that are likely to form a disproportionate amount of SOA relative to other monoterpenes (Lane et al., 2008; Maksymuik et al., 2009; Fry et al., 2011). In a biomass burning plume, extremely high amounts of NMOCs, and organic and inorganic aerosol are simultaneously released creating numerous surface sites for condensation in a highly oxidizing plume environment (OH concentrations can reach  $10^7 \text{ cm}^3 \text{ molec}^{-1} \text{ s}^{-1}$ ; Hobbs et al., 2003; Yokelson et al., 2009). Most research regarding SOA formation from terpenes has been performed in controlled laboratories and/or photochemical chambers where variables such as seed aerosol or oxidant concentration can be varied. Extrapolating chamber results to atmospheric conditions is not simple (Holzinger et al., 2010), but our confirmation of high levels of limonene and other terpenes in smoke plumes could help explain some of the variability in SOA production observed in fire smoke plumes to date (Saathoff et al., 2009; Hennigan et al., 2011; Akagi et al., 2012). It was possible to measure both the sum of monoterpenes by FTIR and/or WAS and the initial OA by AMS on three fires, which yielded mass ratios ( $\Sigma\text{monoterpenes/OA g g}^{-1}$ ) of 0.17, 0.15, and 0.36 (Table 3). The average  $\Sigma\text{monoterpenes/OA}$  ratio measured in this work was 21 % on a mass basis and monoterpenes contributed to only 13.9 % of NMOC on a mass basis. Monoterpenes will not convert 100 % to SOA, and OA evolution in biomass burning plumes may lead to small decreases in OA,

or increases up to a factor of  $\sim 3$  (Hennigan et al., 2011). Thus, unless terpenes are emitted in much greater quantities from other fuel types they likely do not contribute to most of the total variability observed in SOA. Because monoterpenes have 10 carbon atoms (Fig. 7), their oxidation could potentially contribute to a larger share of the variability observed in production of smaller OVOCs downwind (Jacob et al., 2002; Jost et al., 2003; Holzinger et al., 2005, 2010; Yokelson et al., 2008, 2009; Pan et al., 2009; Akagi et al., 2012; Sect 3.7).

### 3.4 C<sub>3</sub>-C<sub>4</sub> alkynes

A recent study was able to assign CO and other air-quality-relevant species observed in the Mexico City area to either biomass burning or urban emissions by assuming that nearly all the HCN was emitted by biomass burning, while ethyne was emitted by both urban sources and fires, but with different ratios to CO (Crouse et al., 2009). Ethyne is emitted in higher proportion to CO by urban sources than by fires and the ethyne from biomass burning is usually produced mostly by flaming combustion (Lobert et al., 1991; Yokelson et al., 2008), with a slower reaction rate with OH than most other hydrocarbons resulting in an atmospheric lifetime of  $\sim 10$ –14 days (Crouse et al., 2009). Because of its emission from multiple combustion sources, ethyne is not an ideal tracer for any one source. Simpson et al. (2011) reported that other alkynes such as propyne have so far only been detected from biomass burning in widespread WAS measurements, making them of interest as possible biomass burning indicators despite having a relatively short lifetime of  $\sim 2$  days. Our study-average  $ER(\Delta\text{propyne}/\Delta\text{CO})$  of  $(4.51 \pm 0.50) \times 10^{-4}$  from the airborne-based platform is 2.5 times greater than the  $ER(\Delta\text{propyne}/\Delta\text{CO})$  reported by Simpson et al. (2011) ( $1.8 \pm 0.8 \times 10^{-4}$ ) at a lower MCE suggesting more smoldering combustion in their study and that propyne may be emitted primarily by flaming combustion. We also observed the emission of higher alkynes (e.g. 1+2-butyne) from all the SC fires by WAS, which further suggests their potential use as biomass burning tracers. Finally, Fig. 8 shows that the three C<sub>3</sub>-C<sub>4</sub> alkynes detected in this work are positively correlated with MCE and thus, like ethyne, are mostly produced by flaming combustion.

### 3.5 Initial emissions of nitrogen species

#### 3.5.1 NH<sub>3</sub>

NH<sub>3</sub> is the most abundant alkaline gas in the atmosphere and is important in neutralizing acidic species in particulate matter (Seinfeld and Pandis, 1998). Biomass burning is an important NH<sub>3</sub> source (Crutzen and Andreae, 1990) and biomass burning emissions of NH<sub>3</sub> are typically strongly negatively correlated with MCE, meaning it is primarily emitted from smoldering combustion. We compare our  $EF(\text{NH}_3)$  from both the air and ground with other  $EF(\text{NH}_3)$

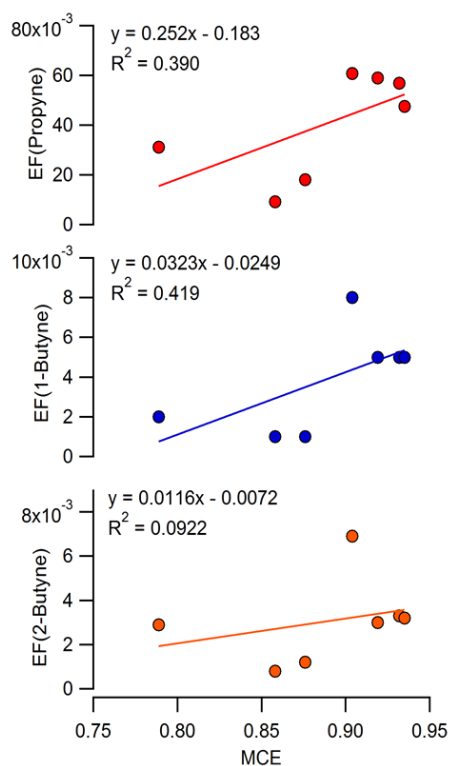


**Fig. 8.** C<sub>3</sub>-C<sub>4</sub> alkyne emission factors ( $\text{g kg}^{-1}$ ) as a function of MCE from the fires in this study measured from airborne and ground-based platforms. The positive correlation of EF with MCE suggests that these alkynes (propyne, 1-butyne, and 2-butyne) are emitted chiefly by flaming combustion processes.

from biomass burning studies of similar fuel types (Fig. 9). A general pattern emerges that the airborne  $EF(\text{NH}_3)$  decrease going from California to Mexico to NC to SC and the ground-based  $EF(\text{NH}_3)$  decrease from NC to SC. Thus, the SC  $EF(\text{NH}_3)$  are systematically lower than observed in other studies of understory fires in pine-dominated forests. Other factors besides MCE can affect ammonia emissions, the most important being the nitrogen content of vegetation (Burling et al., 2010). The nitrogen content tends to be lower in woody biomass (which tends to burn by smoldering combustion) than in foliage (which tends to burn by flaming combustion) (Susott et al., 1996; Burling et al., 2011; Akagi et al., 2011). While the N content of fuels sampled in this work is unknown, this could explain why the regression line fit to the ground-based  $EF(\text{NH}_3)$  (usually of woody biomass, Table 2) lay well below the regression line fit to the airborne  $EF(\text{NH}_3)$  data.

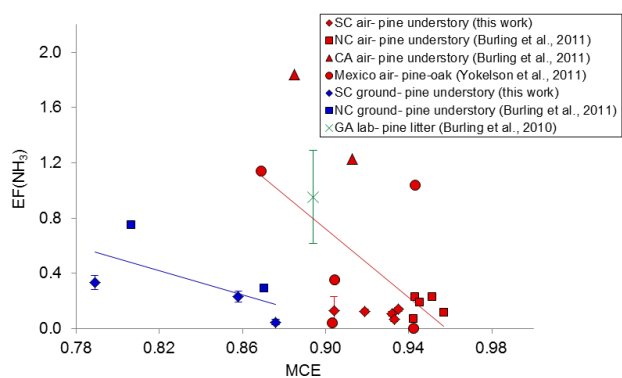


**Fig. 9.**  $EF(NH_3)$  ( $g\ kg^{-1}$ ) as a function of MCE for the South Carolina pine burns of this study (diamonds) measured from both airborne (red) and ground-based (blue) platforms. Error bars ( $1-\sigma$ ) are included for data from this work (error bars from other works are included when available). We also show airborne and ground-based measurements in similar fuels from Burling et al. (2011) (squares), airborne data from Mexican pine-oak forests from Yokelson et al. (2011) (red circles), and pine litter laboratory data from Fort Benning, GA (Burling et al., 2010) (green). Negative correlations of  $EF(NH_3)$  vs. MCE for ground-based (blue line) and airborne (red line) measurements are also shown.

### 3.5.2 HCN

HCN is produced from the pyrolysis of amino acids and is now widely recognized as a useful biomass burning tracer (Li et al., 2003; Crouse et al., 2009). We compare the  $ER(\Delta HCN/\Delta CO)$  from this work to other works in similar fuels, including pine-forest understory burns (Burling et al., 2011), Mexican rural pine-oak forests (Yokelson et al., 2011), Canadian boreal forests (Simpson et al., 2011), and US pine litter from Georgia (Burling et al., 2010) (Fig. 10). We also include ERs from some very different, but globally important fuel types, including savanna fires from Africa (Yokelson et al., 2003b), tropical evergreen deforestation fires from Brazil (Yokelson et al., 2007), peatland (Akagi et al., 2011), and fires in tropical dry forest (Yokelson et al., 2009). The study means for the airborne measurements of  $ER(\Delta HCN/\Delta CO)$  shown in Fig. 10 all fall within the range 0.0063 to 0.0095. The ground-based and lab measurements are lower than this range with the exception of the  $ER(\Delta HCN/\Delta CO)$  from peatland fires, which, at  $0.03 \pm 0.036$ , is more than three times larger than the other values (Akagi et al., 2011). In both this work and Burling et al. (2011), lower HCN emission ratios are observed from a ground-based versus airborne platform when sampling the same fires.

Overall, the airborne and ground-based  $EF(HCN)$  show a strong negative correlation with MCE over a wide MCE range (0.85–0.96), suggesting that HCN was primarily released from smoldering combustion (Fig. 11). This high negative correlation is seen in results from pine-forest organic

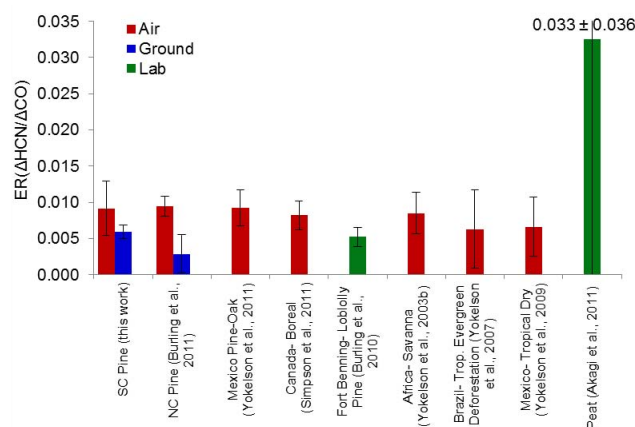


**Fig. 10.** Comparison of  $\Delta HCN/\Delta CO$  study-average emission ratios (mol/mol) measured from airborne (red), ground-based (blue), and laboratory (green) platforms from five North American studies in pine-forest fuels (leftmost bars). We also show four  $ER(\Delta HCN/\Delta CO)$  in other fuel types for comparison. Error bars ( $1-\sigma$ ) are included for all data. The large variation shown for peat is due to a very large value for Indonesian peat that is included in the calculation.

soils collected from Montana, US and the Northwest Territories, Canada (Bertschi et al., 2003). By contrast, airborne  $EF(HCN)$  measured in some other studies of “non-pine” ecosystems are more or less independent of MCE (Yokelson et al., 2003b). Also note in Fig. 11 that the four or five outliers are ground-based data, which may be probing emissions from a different mix of the overall fuel complex. The similarity of study-averaged ERs shown in Fig. 10 and the observation that fire-averaged MCE usually fall in the range of 0.90–0.94 (Fig. 11) confirm that HCN is a useful tracer for the lofted emissions that account for much of the smoke generated by many fires around the world. However, the larger scatter at low MCE in Fig. 11 suggests that HCN may be a better tracer for smoke that is lofted and transported as opposed to smoke that drifts at ground level. Finally, the variability in HCN emissions is magnified when considering a broader range of fuel types. For instance, there are very large  $EF(HCN)$  emissions from peat, while Christian et al. (2010) report that HCN was below FTIR detection limits when sampling cooking fire emissions in both Mexico and Africa.

### 3.5.3 Nitrous Acid (HONO)

HONO is an important precursor for OH radicals in the atmosphere (Broske et al., 2003). Photolysis is the primary daytime fate of HONO and it forms OH and NO within 10–20 min (Schiller et al., 2001). Given the importance of OH as a key atmospheric oxidant, photolysis of HONO could significantly affect the photochemistry of some aging plumes (Alvarado and Prinn, 2009). HONO is now recognized as a major flaming combustion product from fires that has been measured in both lab and field experiments (Trentmann et

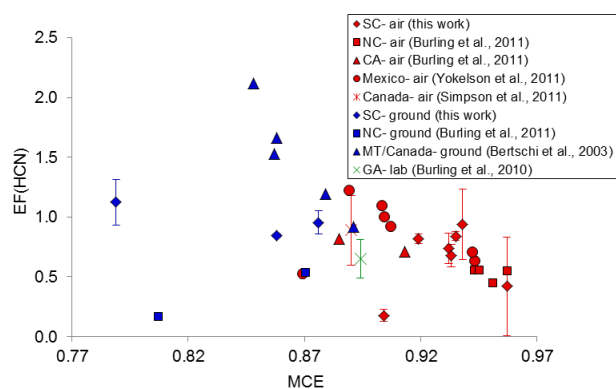


**Fig. 11.** HCN fire-averaged emission factors ( $\text{g kg}^{-1}$ ) as a function of MCE for pine/conifer fuel types measured from airborne (red), ground-based (blue), and laboratory (green) platforms. Error bars ( $1\text{-}\sigma$ ) are included for data from this work (error bars from other works are included when available). The data show a general negative correlation with MCE, however, ground-based data alone have higher variability and less MCE dependence.

al., 2005; Keene et al., 2006; Yokelson et al., 2007, 2009; Burling et al., 2010, 2011). In SC, HONO was detected by AFTIR during four of the seven fires. The measurable  $\Delta\text{HONO}/\Delta\text{NO}_x$  molar ratios ranged from 0.158 to 0.329 with an average of  $0.226 \pm 0.091$ , which is greater than ratios obtained from both laboratory ( $0.109 \pm 0.039$ ) and airborne ( $0.130 \pm 0.045$ ) measurements in NC of fires in pine-forest understory fuels (Burling et al., 2010, 2011). The high  $\Delta\text{HONO}/\Delta\text{NO}_x$  ratios observed for some SC fires confirm that HONO can be a significant part of the initial  $\text{NO}_y$ .

### 3.6 Sulfur containing species

Carbonyl sulfide (OCS) is a known emission from biomass burning and its long tropospheric lifetime of 2–7 yr (Xu et al., 2002) makes it a major non-volcanic source of sulfur to the upper atmosphere (Blake et al., 2004). OCS is ultimately oxidized to  $\text{SO}_2$ , which is usually the main S-containing species emitted by fires (Akagi et al., 2011), but  $\text{SO}_2$  was not measured in this work. We report an OCS ground-based emission factor of  $0.122 \pm 0.187$  (Table 3). The large standard deviation is primarily due to the very high EF measured from the Block 22b fire, which was approximately 20 times greater than EFs measured from Block 6 or Block 9b. We report an average airborne OCS emission factor of  $0.010 \pm 0.003$ . Simpson et al. (2011) report  $\text{EF}(\text{OCS})$  of  $0.029 \pm 0.007$  from Canadian boreal forest fires, which is almost three times higher than our airborne  $\text{EF}(\text{OCS})$  and obtained at lower MCE. Yokelson et al. (1997) measured a high  $\text{EF}(\text{OCS})$  of  $1.63 \pm 3.01$  from boreal peat in the lab. OCS is negatively correlated with MCE (Table 4) making it primarily a smoldering emission. Analogous to nitrogen, sulfur emissions are

highly dependent on fuel sulfur content so the variable EFs reported in literature are not unreasonable.

We also observed dimethyl sulfide emissions. Dimethyl sulfide has a much shorter lifetime ( $\sim 1$  day, Lenschow et al., 1999) compared to OCS, and is quickly oxidized to compounds like  $\text{SO}_2$  during daylight hours. We report  $\text{EF}(\text{DMS})$  of  $0.032 \pm 0.040$  (ground-based) and  $0.008 \pm 0.003$  (airborne). Like the OCS data, we note strong negative correlation with MCE (Table 4), confirming emission of DMS from smoldering and RSC. Simpson et al. (2011) report  $\text{EF}(\text{DMS})$  of  $0.0023 \pm 0.0012$ , which is significantly lower than what was observed in this work.

### 3.7 Plume aging

Complex, highly variable photochemistry can cause large changes in smoke composition within minutes after its initial emission. The photochemistry is strongly influenced by variable factors such as temperature, time of day, humidity, cloud cover, dilution rates, and potential changes in concentration and speciation of the initial emissions at the fire source (Akagi et al., 2012). There are also numerous other chemical and physical processes that can affect fresh smoke as it begins to mix with ambient air, such as mixing with biogenic and/or anthropogenic emissions, cloud processing, coagulation, and gas-to-particle conversion (Reid et al., 1998). In this work we present downwind smoke measurements that help isolate how photochemical processes and a few other factors affect plume chemistry.

Plume aging data were collected from the aircraft on four fires: Block 9b (1 November), Georgetown (7 November), Francis Marion (8 November), and Bamberg (10 November). However, the “useable” data from this study were strongly limited by the low excess mixing ratios in the downwind plumes. For context, in plume aging measurements from a California chaparral fire named the Williams Fire,  $\Delta\text{CO}$  values of  $\sim 350\text{--}937$  ppb were observed after 4.5 h of plume aging (Akagi et al., 2012). In plume aging measurements in South Africa (the Timbavati Fire),  $\Delta\text{CO}$  values of 549–644 ppb were observed after almost an hour of aging (Hobbs et al., 2003). Jost et al. (2003) measured CO levels averaging 417 ppb after approximately 2 h of aging in a Namibian biomass burning plume, where the plume’s extent was defined as the region with CO mixing ratios exceeding 400 ppb. In contrast, in the SC plumes we typically observed a  $\Delta\text{CO}$  of  $\sim 25$  ppb after just 1–1.5 h of aging, except on the Block 9b and Francis Marion fires, which had a few downwind  $\Delta\text{CO}$  near 100 ppb, which is still relatively low. The higher downwind  $\Delta\text{CO}$  values of the Williams Fire occurred mainly because the plume diluted above the mixed layer with minimal vertical mixing. The downwind smoke on the Timbavati Fire was likely more concentrated because that fire burned 20–30 times more area than the SC fires in about the same time, contributing to a stronger source strength. A consequence of the low downwind  $\Delta\text{CO}$  values in SC is a SNR in the downwind

samples that was often 30–40 times lower in SC than at the Williams Fire or Timbavati Fire. Low  $\Delta\text{CO}$  of 25 ppb in downwind samples approaches the uncertainty (natural variability) in background CO (typically 5–6 ppb), and most NMOC species are only present at  $\sim 2 \pm 1\%$  of CO so they are near or below our AFTIR detection limit of  $\sim 1$  ppb for most species. In summary, we obtained good downwind CO and O<sub>3</sub> data in all downwind plumes, but with the exception of methanol and formaldehyde on the Block 9b and Francis Marion fires, downwind AFTIR NMOC mixing ratios were near or below our limit of detection and prevent us from presenting well-supported conclusions. Many other species such as CH<sub>3</sub>COOH and PAN were measured downwind and consistently increased in the downwind smoke, however, due to the high uncertainty in the NEMRs we do not report the data. The WAS technique is more sensitive than AFTIR, but we were only able to obtain one downwind WAS sample. Also worth noting is the high background CO during this study. Whereas the Williams Fire and Timbavati Fire were in remote locations and had relatively low background CO levels of  $\sim 100$  ppb, the SC fires show average background CO mixing ratios of 170–250 ppb and were sometimes located near major urban centers, suggesting the presence of urban emissions and the inevitability of biomass burning/fossil fuel (BB/FF) mixing scenarios.

Another concern was identifying which downwind samples were pseudo-Lagrangian. We estimated the emission time of each downwind sample by subtracting the calculated time since emission from the time the downwind sample was collected. If the aircraft was sampling the source of the fire at the estimated emission time of the downwind sample and the plume was well-mixed at the source, we then have initial ERs that represent the starting chemistry of the downwind sample and it was classified as pseudo-Lagrangian. Further, for each fire in SC, the ERs did not exhibit significant increasing or decreasing trends during our source sampling period so we took the fire-averaged ER as our best guess of the starting ER for all pseudo-Lagrangian downwind samples. When a downwind sample was emitted before or after we were at the source, the fire-averaged ER is still our best estimate of the starting ER to compare to the downwind NEMRs, but that guess is less strongly supported because of the greater possibility that the initial smoke chemistry was different when we were not sampling the source. To make this distinction in confidence clear, all downwind samples from all flights that were pseudo-Lagrangian are shown as solid circles and those samples that were emitted when we were not sampling at the fire source are considered non-Lagrangian and shown as open circles in Figs. 12, 14, and 15. Additionally, in these figures simplified trends in NEMR are shown as linear trendlines for some fires because they empirically fit the data. We do not suggest that these linear relationships can be rigorously derived from the complex, often unknown, underlying chemistry.

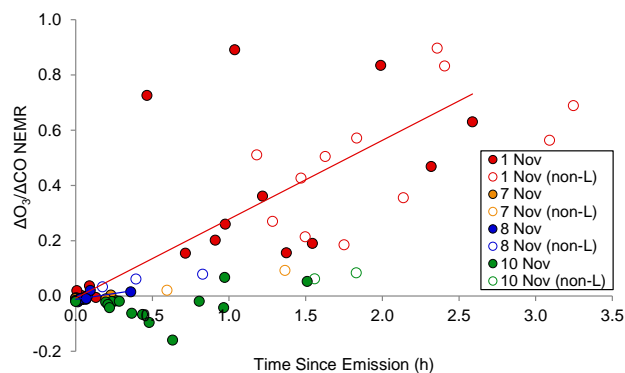


**Fig. 12.**  $\Delta\text{O}_3/\Delta\text{CO}$  NEMR vs. time since emission ( $h$ ). Airborne measurements were collected up to  $\sim 2.5$  h downwind. All the SC fires that we were able to collect downwind data on are shown: Block 9b (1 November, red), Georgetown (7 November, orange), Francis Marion (8 November, blue), and Bamberg (10 November, green). The y-intercept of the trendlines for 1 and 8 November is forced to the average  $\Delta\text{O}_3/\Delta\text{CO}$  NEMR at time  $t = 0$  h for each fire. All trendlines represent only pseudo-Lagrangian data points. The 7 November data did not have enough points to constrain a line and the 10 November data was clearly non-linear. Solid circles reflect data that were Lagrangian while open circles labeled “non-L” represent non-Lagrangian samples collected on that respective day.

### 3.7.1 Ozone

In Fig. 12 we show downwind ozone data from the Block 9b, Georgetown, Francis Marion, and Bamberg fires (on 1 November, 7 November, 8 November, and 10 November, respectively). Our most aged plume samples were collected from the Block 9b fire. Conditions were favorable for ozone formation with clear skies. Although variability in the  $\Delta\text{O}_3/\Delta\text{CO}$  NEMR is high on this day (e.g. a 15–90 % range at 1.5 h), pseudo-Lagrangian and non-Lagrangian points basically follow the same trend suggesting about 70 %  $\Delta\text{O}_3/\Delta\text{CO}$  after 2.5 h, which is the fastest ozone formation that has been measured in a biomass burning plume to our knowledge. An additional feature of interest from the Block 9b fire is the low initial NO<sub>x</sub> ER to CO ( $\sim 0.01$ ). Ozone production in biomass burning plumes is normally NO<sub>x</sub> limited downwind and so low initial NO<sub>x</sub> would suggest minimal O<sub>3</sub> formation downwind. However, the Block 9b plume, though clearly composed primarily of biomass burning smoke, was sampled downwind after transport over a region including part of the metropolitan Columbia area (population  $\sim 748\,000$ ), a large natural gas power plant, and an airport (Fig. 3). The Fort Jackson base may have some significant NO<sub>x</sub> sources and certainly non-fire NO<sub>x</sub> sources would have been encountered once the smoke plume reached the location of the powerplant (when the Block 9b smoke had aged approximately 1 h). Our “raw”  $\Delta\text{NO}_x/\Delta\text{CO}$  levels seemed to surge at the location of the power plant, but unfortunately the NO<sub>x</sub> values were near or below our detection

limit due to rapid dilution and so  $\Delta\text{NO}_x/\Delta\text{CO}$  plume aging data is not presented here. The sole downwind WAS canister was collected just upwind of the power plant and was unfortunately not optimum for estimating the extent of mixing. Nonetheless, we believe that the plume mixed with air that contained fresh NO<sub>x</sub> from fossil fuel sources and that the rapid ozone formation we observed was due in part to BB/FF mixing. Lee et al. (2008), Singh et al. (2010), and Jacob et al. (2010) have also reported an increase in ozone formation rates when biomass burning emissions are mixed with urban emissions.

The Georgetown and Francis Marion fires were on sunny days and in rural areas with no obvious sources of fossil fuel emissions to mix with. We observed up to  $\sim 1.5\%$   $\Delta\text{O}_3/\Delta\text{CO}$  in less than 30 min and increases to 8% in 50 min if non-Lagrangian samples are considered. This formation rate is considerably slower than that observed from the Block 9b fire, but similar to the O<sub>3</sub> formation rate observed in tropical plumes in Africa and Mexico (Yokelson et al., 2003b, 2009); and it is also over 4 times faster than the  $\sim 10\%$   $\Delta\text{O}_3/\Delta\text{CO}$  observed in 4.5 h in the Williams Fire (Akagi et al., 2012). The Bamberg fire smoke plume had the slowest ozone formation of our SC fires with less than 10%  $\Delta\text{O}_3/\Delta\text{CO}$  after 2 h. This fire was on a cloudy day with no notable BB/FF plume mixing, two factors which likely slowed down plume photochemistry. Ozone destruction dominated over ozone formation resulting in a net loss of ozone during the first 30–45 min of plume aging. This is likely due to the rapid reaction of ozone with NO or possibly with NMOCs or particles. While this is the slowest O<sub>3</sub> formation observed in SC, we note that the  $\Delta\text{O}_3/\Delta\text{CO}$  at the end of the aging measurements was similar to that observed in the Williams Fire.

Figure 13 compares the first few hours of ozone formation in SC with two other studies discussed above: Akagi et al. (2012) who observed  $\Delta\text{O}_3/\Delta\text{CO}$  NEMR increases up to  $\sim 10\%$  over the course of 4.5 h, and Yokelson et al. (2009) who measured a rapid increase in  $\Delta\text{O}_3/\Delta\text{CO}$  to  $\sim 15\%$  in less than 1 h from a plume in the Yucatan. In context, O<sub>3</sub> formation is probably ubiquitous in tropical biomass burning plumes, but O<sub>3</sub> destruction, as well as formation at many different rates, can occur in extratropical plumes (Andreae et al., 1994; Akagi et al., 2011; Jaffe and Wigder, 2012). For example, de Gouw et al. (2006) saw little to no O<sub>3</sub> formation in Alaskan plumes, while Goode et al. (2000) observed an ozone rise to 9% in  $\sim 2$  h in an Alaskan plume, and Hobbs et al. (1996) reported 1.5%  $\Delta\text{O}_3/\Delta\text{CO}$  in 30 min in a plume in the Pacific Northwest. Nine plumes from boreal wildfires that were 6–15 days old were sampled in the Azores in 2004 and 8 of the plumes had  $\Delta\text{O}_3/\Delta\text{CO}$  ranging from 9% to 89% (Val Martin et al., 2006; Lapina et al., 2006). The  $\Delta\text{O}_3/\Delta\text{CO}$  NEMRs observed in the Azores are similar to the NEMRs observed in our SC work, but we observed the  $\Delta\text{O}_3/\Delta\text{CO}$  levels in  $\sim 2.5$  h compared with 6–15 days. Our study-average  $\Delta\text{O}_3/\Delta\text{CO}$  is  $\sim 60\%$  in 2.5 h. As mentioned

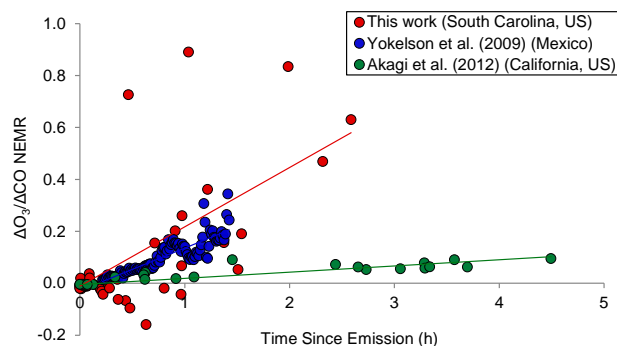


**Fig. 13.**  $\Delta\text{O}_3/\Delta\text{CO}$  vs. time since emission from this study (red), Yokelson et al. (2009) (blue), and Akagi et al. (2012) (green).

above, the highest ozone formation rates observed in SC are likely linked to mixing with urban emissions, a plume mixing scenario that is expected to be widespread globally. Measurements of secondary production of O<sub>3</sub> and other species in biomass burning plumes from ground stations, aircraft, and remote sensing are all important for validating models and assessing the contribution of biomass burning to tropospheric O<sub>3</sub> (Fishman et al., 2003; Sudo and Akimoto, 2007; Wu et al., 2007).

### 3.7.2 Methanol

In previous pseudo-Lagrangian measurements of biomass burning plume evolution the methanol to CO ratio was stable or slowly decreased (e.g. Goode et al., 2000) in the first few hours. In non-Lagrangian measurements mixed results have been obtained.  $\Delta\text{CH}_3\text{OH}/\Delta\text{CO}$  decreased rapidly in a cloud-processed biomass burning plume (Yokelson et al., 2003b; Tabazadeh et al., 2004). In contrast, Holzinger et al. (2005) measured NEMRs for  $\Delta\text{CH}_3\text{OH}/\Delta\text{CO}$  and  $\Delta\text{C}_3\text{H}_6\text{O}/\Delta\text{CO}$  in biomass burning plumes several days old that were enhanced by factors of 2–6 and 2–14, respectively, above their estimate of the literature average ERs for these species. In this study, in both fires with sufficient downwind SNR (Block 9b and Francis Marion burns), we observe a post-emission increase in  $\Delta\text{CH}_3\text{OH}/\Delta\text{CO}$ , which confirms that methanol may sometimes be the oxidation product of co-emitted NMOC. The rates of methanol formation downwind are variable (Fig. 14). The Block 9b fire shows a  $\Delta\text{CH}_3\text{OH}/\Delta\text{CO}$  increase from 0.013 to  $\sim 0.024$  over 2 h following emission, an increase of a factor of 1.7. The Lagrangian and non-Lagrangian data support the same general linear trend (though with high scatter), which suggests that the source ERs were relatively stable over most of the fire lifetime. On the Francis Marion fire we observed an even larger increase in  $\Delta\text{CH}_3\text{OH}/\Delta\text{CO}$ : from 0.012 up to  $\sim 0.030$  within the first half hour, or an increase by a factor of 2.4. Taken together with past work, these new SC results suggest that post-emission trends in methanol are highly variable

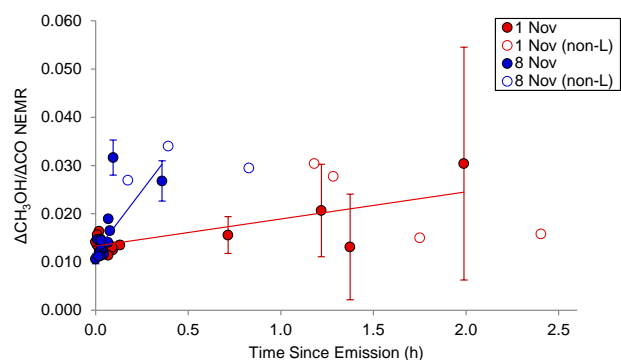


**Fig. 14.**  $\Delta\text{CH}_3\text{OH}/\Delta\text{CO}$  vs. time since emission ( $h$ ). Airborne measurements were collected up to  $\sim 2.5$  h downwind. Fires on which we were able to collect downwind data with good SNR, Block 9b (1 November, red) and Francis Marion (8 November, blue), are included here. The y-intercept of the trendlines is forced to the average  $\text{ER}(\text{CH}_3\text{OH})$  at time  $t = 0$  for each fire. Solid circles reflect data that were considered Lagrangian while open circles labeled “non-L” represent non-Lagrangian samples collected on that respective day. Vertical error bars reflect instrument uncertainty in methanol (500 ppt).

and likely due to large differences in the initial emissions of precursors. Specifically, in this study, the rapid methanol increases could stem in part from the oxidation of monoterpenes, which may have been emitted at higher than average levels in the SC fires (Yokelson et al., 2013). If all the initial monoterpenes measured from the Francis Marion fire reacted to form methanol, we would observe an increase in  $\Delta\text{CH}_3\text{OH}/\Delta\text{CO}$  of  $\sim 0.032$ , compared to the observed increase in  $\Delta\text{CH}_3\text{OH}/\Delta\text{CO}$  of  $\sim 0.018$ . While it is highly unlikely that  $\sim 56\%$  of monoterpene photo-oxidation products end up as methanol, there are sufficient monoterpene emissions to cause a large part of the increase in  $\Delta\text{CH}_3\text{OH}/\Delta\text{CO}$ . Furthermore, the initial “total” amount of monoterpenes from Francis Marion quoted above was due solely to limonene, as other monoterpenes were not measured on this fire, but were likely present (AFTIR could only specifically retrieve limonene). Thus, we would expect the actual  $\text{ER}(\Sigma\text{monoterpenes}/\text{CO})$  to be significantly higher. In summary, while the mechanism for methanol formation remains speculative, this work confirms that secondary production can sometimes be significant compared with primary emission. Secondary production of methanol, if common, would suggest a larger biomass burning contribution to the global methanol budget, but clearly biogenic emissions would still be the dominant source (Jacob et al., 2005).

### 3.7.3 Formaldehyde

We also observed large increases in  $\Delta\text{HCHO}/\Delta\text{CO}$  within  $\sim 2$  h following emission in SC (Fig. 15). On the Block 9b fire  $\Delta\text{HCHO}/\Delta\text{CO}$  increased from 0.022 to 0.075 (a factor

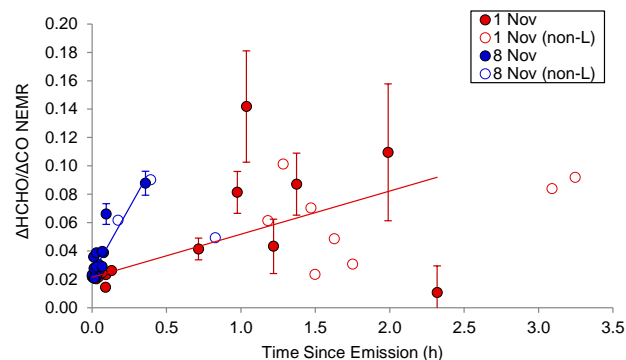


**Fig. 15.**  $\Delta\text{HCHO}/\Delta\text{CO}$  vs. time since emission ( $h$ ). Airborne measurements were collected up to  $\sim 2.5$  h downwind. Fires with good downwind data, Block 9b (1 November, red) and Francis Marion (8 November, blue), are included here. The y-intercept of the trendlines is forced to the average  $\text{ER}(\text{HCHO})$  at time  $t = 0$  for each fire. Solid circles reflect data that were considered Lagrangian while open circles labeled “non-L” represent non-Lagrangian samples collected on that respective day. Vertical error bars reflect instrument uncertainty in formaldehyde (1 ppb).

of 3.5) in just under 2.5 h. On the Francis Marion fire we observed an immediate, sharp increase in  $\Delta\text{HCHO}/\Delta\text{CO}$  from 0.024 to 0.089 (a factor of  $\sim 3.7$ ) in under 30 min. These increases are larger than previously reported in pseudo-Lagrangian measurements (e.g. Akagi et al., 2012) although a similar increase was measured by the NCAR formaldehyde instrument, but not reported in Yokelson et al. (2009). The downwind  $\Delta\text{CO}$  from the Francis Marion fire were all above  $\sim 120$  ppb and the samples shown all have  $\Delta\text{HCHO}$  well above the 1 ppb formaldehyde detection limit, suggesting that these dramatic increases are accurately measured. Formaldehyde is an important source of OH in biomass burning plumes (Mason et al., 2001) that can be formed via oxidation of many reactive NMOCs. For instance, it is a known product of monoterpene oxidation and has been observed from  $\alpha$ -pinene ozonolysis and limonene oxidation via OH (Capouet et al., 2004; Muller et al., 2005). Clearly NMOCs in addition to terpenes also need to contribute to explain HCHO increases as large as we observed. On the other hand, formaldehyde is also lost by photolysis and reaction with OH or  $\text{HO}_2$ . Thus, formaldehyde, and by extension OH, will be at levels heavily influenced by the particular mix of many co-emitted NMOCs.

## 4 Conclusions

The final phase of our study of southeastern US prescribed fire emissions succeeded in greatly expanding the range of weather and fuel conditions probed and the scope of smoke chemistry measurements collected. Our previous work measured the prescribed fire emissions in intensively managed loblolly pine stands during a wet spring (February–March

2010). The new results reported here include emissions measurements for relatively undisturbed longleaf pine stands during a dry fall (October–November 2011). The emission factors (EF) measured in 2011 differ by ~13–195 % from the EF measured in 2010 for numerous organic and N-containing species, even though both phases of the study were conducted in ecosystems that are nominally “the same” in many simplified global vegetation schemes. Thus, taken together, the 2010 and 2011 results now give a much improved picture of the mean and variability in emissions for prescribed fires in southeastern US pine-forest understory fuels. However, much work would be needed to develop an ability to predict the emissions a priori from individual fires of this type with uncertainties significantly smaller than the range in EF we observed. For now, the emission factors measured in this study and other recent studies (Yokelson et al., 2013) have been used to update a global emission factor database described by Akagi et al. (2011) with updates available at: <http://bai.acd.ucar.edu/Data/fire/>.

The expanded suite of measurements produced emission factors for up to 97 trace gas species from seven prescribed fires – from both airborne and ground-based platforms. The measurements include fire-averaged emission factors for a large suite of terpene compounds emitted by wildland fires for the first time. Limonene and  $\alpha$ -pinene were the dominant terpenes emitted.  $\beta$ -Pinene, 4-carene, myrcene, camphene, and isoprene were also measured and the sum of monoterpenes accounted for 0.4–27.9 % of initial NMOC mass and equaled ~21 % of OA mass. An assessment of likely smoke plume photochemistry indicates that monoterpenes emitted by fires would react mainly with OH during the day and NO<sub>3</sub> at night. The known photochemistry of the terpenes and their measured initial abundance suggests that they contributed to our observations of secondary formation of small organic trace gases in the first few hours of post-emission plume aging. For example, we report the first pseudo-Lagrangian measurements of methanol formation in the downwind plumes (an approximate doubling) and also the largest post-emission increases in formaldehyde published to date (an approximate tripling). The observed monoterpenes are known precursors of methanol and formaldehyde, but the large amount of secondary VOCs suggests that other NMOCs, both measured and unmeasured, also acted as precursors. If secondary methanol production in biomass burning plumes is common, then the global methanol source from biomass burning should be scaled upwards. In contrast to the high variability in NMOC emissions, the  $\Delta$ HCN/ $\Delta$ CO emission ratio fell within a fairly narrow range that included the  $\Delta$ HCN/ $\Delta$ CO ratio for fires in many other ecosystems. This further confirms the value of HCN as a biomass burning indicator/tracer. Our results also support an earlier finding that C<sub>3</sub>–C<sub>4</sub> alkynes may be of use as biomass burning indicators on the time-scale of hours to a day. It was possible to measure the photochemical production of ozone in four of the plumes. Slower O<sub>3</sub> production was observed on a cloudy day with low co-

emissions of NO<sub>x</sub> and the fastest O<sub>3</sub> production was observed on a sunny day when the plume almost certainly incorporated significant additional NO<sub>x</sub> by passing over the Columbia, SC metropolitan area. In the mixed BB/FF plume  $\Delta$ O<sub>3</sub>/ $\Delta$ CO reached levels of 10–90 % within one hour and total O<sub>3</sub> was as high as 104 ppb. With population increasing both in the southeastern US and in developing countries where biomass burning is common, the aggressive ozone increase in mixed emissions could be an increasingly significant public health issue.

*Acknowledgements.* This work was supported by the Strategic Environmental Research and Development Program (SERDP) project RC-1649 and administered partly through Forest Service Research Joint Venture Agreement 08JV11272166039, and we thank the sponsors for their support. CSU was supported by Joint Fire Science Program grant #11-1-5-12. Shawn Urbanski and some of the Twin Otter flight hours were supported by Joint Fire Science Program grant #08-1-6-09. We appreciate the efforts of Aaron Sparks and Signe Leirfallom to measure the consumption of wildland fuels for this study. Adaptation of the USFS Twin Otter for research flights was supported primarily by NSF grant ATM 0513055. Special thanks to our pilot Bill Mank and Twin Otter mechanic Steve Woods. We thank Holly Eissing for constructing maps of Fort Jackson flight tracks, hot spots, and fire locations shown in Figs. 2, 3, 4. We greatly appreciate the collaboration and efforts of John Maitland and forestry staff at Fort Jackson and we thank the Columbia dispatch office of the South Carolina Forestry Commission for assistance in locating fires to sample.

Edited by: T. Bertram

## References

- Akagi, S. K., Yokelson, R. J., Wiedinmyer, C., Alvarado, M. J., Reid, J. S., Karl, T., Crounse, J. D., and Wennberg, P. O.: Emission factors for open and domestic biomass burning for use in atmospheric models, *Atmos. Chem. Phys.*, 11, 4039–4072, doi:10.5194/acp-11-4039-2011, 2011.
- Akagi, S. K., Craven, J. S., Taylor, J. W., McMeeking, G. R., Yokelson, R. J., Burling, I. R., Urbanski, S. P., Wold, C. E., Seinfeld, J. H., Coe, H., Alvarado, M. J., and Weise, D. R.: Evolution of trace gases and particles emitted by a chaparral fire in California, *Atmos. Chem. Phys.*, 12, 1397–1421, doi:10.5194/acp-12-1397-2012, 2012.
- Alvarado, M. J. and Prinn, R. G.: Formation of ozone and growth of aerosols in young smoke plumes from biomass burning: 1. Lagrangian parcel studies, *J. Geophys. Res.*, 114, D09306, doi:10.1029/2008JD011144, 2009.
- Andreae, M. O., Anderson, B. E., Blake, D. R., Bradshaw, J. D., Collins, J. E., Gergory, G. L., Sachse, G. W., and Shipham, M. C.: Influence of plumes from biomass burning on atmospheric chemistry over the equatorial and tropical South Atlantic during CITE 3, *J. Geophys. Res.*, 99, 12793–12808, doi:10.1029/94JD00263, 1994.
- Bertschi, I. T., Yokelson, R. J., Ward, D. E., Babbitt, R. E., Su-sott, R. A., Goode, J. G., and Hao, W. M.: Trace gas and particle

- emissions from fires in large diameter and belowground biomass fuels, *J. Geophys. Res.*, 108, 8472, doi:10.1029/2002JD002100, 2003.
- Beswick, K. M., Gallagher, M. W., Webb, A. R., Norton, E. G. and Perry, F.: Application of the Aventech AIMMS20AQ airborne probe for turbulence measurements during the Convective Storm Initiation Project, *Atmos. Chem. Phys.*, 8, 5449–5463, doi:10.5194/acp-8-5449-2008, 2008.
- Biswell, H. H.: Prescribed burning in California wildlands vegetation management, Berkeley, CA: University of California Press, 255 pp., 1989.
- Blake, N. J., Streets, D. G., Woo, J.-H., Simpson, I. J., Green, J., Meinardi, S., Kita, K., Atlas, E., Fuelberg, H. E., Sachse, G., Avery, M. A., Vay, S. A., Talbot, R. W., Dibb, J. E., Bandy, A. R., Thornton, D. C., Rowland, F. S., and Blake, D. R.: Carbonyl sulfide and carbon disulfide: Large-scale distributions over the western Pacific and emissions from Asia during TRACE-P, *J. Geophys. Res.*, 109, D15S05, doi:10.1029/2003JD004259, 2004.
- Bond, T. C., Streets, D. G., Yarber, K. F., Nelson, S. M., Woo, J., and Klimont, Z.: A technology-based global inventory of black and organic carbon emissions from combustion, *J. Geophys. Res.*, 109, D14203, doi:10.1029/2003JD003697, 2004.
- Bouvier-Brown, N. C., Holzinger, R., Palitzsch, K., and Goldstein, A. H.: Large emissions of sesquiterpenes and methyl chavicol quantified from branch enclosure measurements, *Atmos. Environ.*, 43, 389–401, 2009.
- Bröske, R., Kleffmann, J., and Wiesen, P.: Heterogeneous conversion of NO<sub>2</sub> on secondary organic aerosol surfaces: A possible source of nitrous acid (HONO) in the atmosphere?, *Atmos. Chem. Phys.*, 3, 469–474, doi:10.5194/acp-3-469-2003, 2003.
- Burling, I. R., Yokelson, R. J., Griffith, D. W. T., Johnson, T. J., Veres, P., Roberts, J. M., Warneke, C., Urbanski, S. P., Reardon, J., Weise, D. R., Hao, W. M., and de Gouw, J.: Laboratory measurements of trace gas emissions from biomass burning of fuel types from the southeastern and southwestern United States, *Atmos. Chem. Phys.*, 10, 11115–11130, doi:10.5194/acp-10-11115-2010, 2010.
- Burling, I. R., Yokelson, R. J., Akagi, S. K., Urbanski, S. P., Wold, C. E., Griffith, D. W. T., Johnson, T. J., Reardon, J., and Weise, D. R.: Airborne and ground-based measurements of the trace gases and particles emitted by prescribed fires in the United States, *Atmos. Chem. Phys.*, 11, 12197–12216, doi:10.5194/acp-11-12197-2011, 2011.
- Canagaratna, M. R., Jayne, J. T., Jimenez, J. L., Allan, J. D., Alfarra, M. R., Zhang, Q., Onasch, T. B., Drewnick, F., Coe, H., Middlebrook, A., Delia, A., Williams, L. R., Trimborn, A. M., Northway, M. J., DeCarlo, P. F., Kolb, C. E., Davidovits, P., and Worsnop, D. R.: Chemical and microphysical characterization of ambient aerosols with the Aerodyne aerosol mass spectrometer, Edited by A. Viggiano, *Mass Spectrom. Rev.*, 26, 185–222, 2007.
- Capouet, M., Peeters, J., Nozière, B., and Müller, J.-F.: Alpha-pinene oxidation by OH: simulations of laboratory experiments, *Atmos. Chem. Phys.*, 4, 2285–2311, doi:10.5194/acp-4-2285-2004, 2004.
- Carter, M. C. and Foster, C. D.: Prescribed burning and productivity in southern pine forests: a review, *Forest Ecol. Manage.*, 191, 93–109, 2004.
- Christian, T., Kleiss, B., Yokelson, R. J., Holzinger, R., Crutzen, P. J., Hao, W. M., Saharjo, B. H., and Ward, D. E.: Comprehensive laboratory measurements of biomass-burning emissions: 1. Emissions from Indonesian, African, and other fuels, *J. Geophys. Res.*, 108, 4719, doi:10.1029/2003JD003704, 2003.
- Christian, T. J., Yokelson, R. J., Carvalho Jr., J. A., Griffith, D. W. T., Alvarado, E. C., Santos, J. C., Neto, T. G. S., Veras, C. A. G., and Hao, W. M.: The tropical forest and fire emissions experiment: Trace gases emitted by smoldering logs and dung from deforestation and pasture fires in Brazil, *J. Geophys. Res.*, 112, D18308, doi:10.1029/2006JD008147, 2007.
- Christian, T. J., Yokelson, R. J., Cárdenas, B., Molina, L. T., Engling, G., and Hsu, S.-C.: Trace gas and particle emissions from domestic and industrial biofuel use and garbage burning in central Mexico, *Atmos. Chem. Phys.*, 10, 565–584, doi:10.5194/acp-10-565-2010, 2010.
- Cochrane, M. A., Moran, C. J., Wimberly, M. C., Baer, A. D., Finney, M. A., Beckendorf, K. L., Eidenshink, J., and Zhu, Z.: Estimation of wildfire size and risk changes due to fuels treatments, *Int. J. of Wildland Fire*, 21, 357–367, 2012.
- Crounse, J. D., DeCarlo, P. F., Blake, D. R., Emmons, L. K., Campos, T. L., Apel, E. C., Clarke, A. D., Weinheimer, A. J., McCabe, D. C., Yokelson, R. J., Jimenez, J. L., and Wennberg, P. O.: Biomass burning and urban air pollution over the Central Mexican Plateau, *Atmos. Chem. Phys.*, 9, 4929–4944, doi:10.5194/acp-9-4929-2009, 2009.
- Crutzen, P. J. and Andreae, M. O.: Biomass burning in the tropics: Impact on atmospheric chemistry and biogeochemical cycles, *Science*, 250, 1669–1678, 1990.
- de Gouw, J. A., Warneke, C., Stohl, A., Wollny, A. G., Brock, C. A., Cooper, O. R., Holloway, J. S., Trainer, M., Fehsenfeld, F. C., Atlas, E. L., Donnelly, S. G., Stroud, V., and Lueb, A.: Volatile organic compounds composition of merged and aged forest fire plumes from Alaska and western Canada, *J. Geophys. Res.*, 111, D10303, doi:10.1029/2005JD006175, 2006.
- Drewnick, F., Hings, S. S., DeCarlo, P., Jayne, J. T., Gonin, M., Fuhrer, K., Weimer, S., Jimenez, J. L., Demerjian, K. L., Borrmann, S., and Worsnop, D. R.: A new Time-of-Flight Aerosol Mass Spectrometer (TOF-AMS) – instrument description and first field deployment, *Aerosol Sci. Tech.*, 39, 637–658, 2005.
- Finlayson-Pitts, B. J. and Pitts Jr., J. N.: Chemistry of the Upper and Lower Atmosphere, Academic Press., San Diego, USA, p. 583, 1040, 2000.
- Fishman, J., Wozniak, A. E., and Creilson, J. K.: Global distribution of tropospheric ozone from satellite measurements using the empirically corrected tropospheric ozone residual technique: Identification of the regional aspects of air pollution, *Atmos. Chem. Phys.*, 3, 893–907, doi:10.5194/acp-3-893-2003, 2003.
- Fry, J. L., Kiendler-Scharr, A., Rollins, A. W., Brauers, T., Brown, S. S., Dorn, H.-P., Dubé, W. P., Fuchs, H., Mensah, A., Rohrer, F., Tillmann, R., Wahner, A., Wooldridge, P. J., and Cohen, R. C.: SOA from limonene: role of NO<sub>3</sub> in its generation and degradation, *Atmos. Chem. Phys.*, 11, 3879–3894, doi:10.5194/acp-11-3879-2011, 2011.
- Goode, J. G., Yokelson, R. J., Ward, D. E., Susott, R. A., Babbitt, R. E., Davies, M. A., and Hao, W. M.: Measurements of excess O<sub>3</sub>, CO<sub>2</sub>, CO, CH<sub>4</sub>, C<sub>2</sub>H<sub>4</sub>, C<sub>2</sub>H<sub>2</sub>, HCN, NO, NH<sub>3</sub>, HCOOH, CH<sub>3</sub>COOH, HCHO, and CH<sub>3</sub>OH in 1997 Alaskan biomass burning plumes by airborne Fourier transform infrared spectroscopy (AFTIR), *J. Geophys. Res.*, 105, 22147–22166, doi:10.1029/2000JD900287, 2000.

- Griffin, R. J., Cocker III, D. R., and Seinfeld, J. H.: Estimate of global atmospheric organic aerosol from oxidation of biogenic hydrocarbons, *Geophys. Res. Lett.*, 26, 2721–2724, 1999.
- Griffith, D. W. T.: Synthetic calibration and quantitative analysis of gas-phase FTIR spectra, *Appl. Spectrosc.*, 50, 59–70, 1996.
- Guenther, A., Karl, T., Harley, P., Wiedinmyer, C., Palmer, P. I., and Geron, C.: Estimates of global terrestrial isoprene emissions using MEGAN (Model of Emissions of Gases and Aerosols from Nature), *Atmos. Chem. Phys.*, 6, 3181–3210, doi:10.5194/acp-6-3181-2006, 2006.
- Hamilton, J. F., Rami Alfarra, M., Wyche, K. P., Ward, M. W., Lewis, A. C., McFiggans, G. B., Good, N., Monks, P. S., Carr, T., White, I. R., and Purvis, R. M.: Investigating the use of secondary organic aerosol as seed particles in simulation chamber experiments, *Atmos. Chem. Phys.*, 11, 5917–5929, doi:10.5194/acp-11-5917-2011, 2011.
- Hanst, P. L., Spiller, L. L., Watts, D. M., Spence, J. W., and Miller, M. F.: Infrared measurements of fluorocarbons, carbon tetrachloride, carbonyl sulfide and other atmospheric trace gases, *Journal of the Air Pollution Control Association*, 25, 1220–1226, 1975.
- Hardy, C. C., Ottmar, R. D., Peterson, J. L., Core, J. E., and Seamon, P.: Smoke management guide for prescribed and wildland fire; 2001 ed., PMS 420-2, National Wildfire Coordinating group, Boise, ID. 226 pp., 2001.
- Hennigan, C. J., Miracolo, M. A., Engelhart, G. J., May, A. A., Presto, A. A., Lee, T., Sullivan, A. P., McMeeking, G. R., Coe, H., Wold, C. E., Hao, W.-M., Gilman, J. B., Kuster, W. C., de Gouw, J., Schichtel, B. A., J. L. Collett Jr., Kreidenweis, S. M., and Robinson, A. L.: Chemical and physical transformations of organic aerosol from the photo-oxidation of open biomass burning emissions in an environmental chamber, *Atmos. Chem. Phys.*, 11, 7669–7686, doi:10.5194/acp-11-7669-2011, 2011.
- Hobbs, P. V., Reid, J. S., Herring, J. A., Nance, J. D., Weiss, R. E., Ross, J. L., Hegg, D. A., Ottmar, R. D., and Lioussé, C.: Particle and trace-gas measurements in smoke from prescribed burns of forest products in the Pacific Northwest. Paper presented at the Biomass Burning and Global Change, Vol. 1, New York, USA, 1996.
- Hobbs, P. V., Sinha, P., Yokelson, R. J., Christian, T. J., Blake, D. R., Gao, S., Kirchstetter, T. W., Novakov, T., and Pilewskie, P.: Evolution of gases and particles from a savanna fire in South Africa, *J. Geophys. Res.*, 108, 8485, doi:10.1029/2002JD002352, 2003.
- Holzinger, R., Williams, J., Salisbury, G., Klüpfel, T., de Reus, M., Traub, M., Crutzen, P. J., and Lelieveld, J.: Oxygenated compounds in aged biomass burning plumes over the Eastern Mediterranean: evidence for strong secondary production of methanol and acetone, *Atmos. Chem. Phys.*, 5, 39–46, doi:10.5194/acp-5-39-2005, 2005.
- Holzinger, R., Williams, J., Herrmann, F., Lelieveld, J., Donahue, N. M., and Röckmann, T.: Aerosol analysis using a Thermal-Desorption Proton-Transfer-Reaction Mass Spectrometer (TD-PTR-MS): a new approach to study processing of organic aerosols, *Atmos. Chem. Phys.*, 10, 2257–2267, doi:10.5194/acp-10-2257-2010, 2010.
- Jacob, D. J., Field, B. D., Jin, E. M., Bey, I., Li, Q., Logan, J. A., Yantosca, R. M., and Singh, H. B.: Atmospheric budget of acetone, *J. Geophys. Res.*, 107, 4110, doi:10.1029/2001JD000694, 2002.
- Jacob, D. J., Field, B. D., Li, Q., Blake, D. R., de Gouw, J., Warneke, C., Hansel, A., Wisthaler, A., Singh, H. B., and Guenther, A.: Global budget of methanol: Constraints from atmospheric observations, *J. Geophys. Res.*, 110, D08303, doi:10.1029/2004JD005172, 2005.
- Jacob, D. J., Crawford, J. H., Maring, H., Clarke, A. D., Dibb, J. E., Emmons, L. K., Ferrare, R. A., Hostetler, C. A., Russell, P. B., Singh, H. B., Thompson, A. M., Shaw, G. E., McCauley, E., Pederson, J. R., and Fisher, J. A.: The Arctic Research of the Composition of the Troposphere from Aircraft and Satellites (ARCTAS) mission: design, execution, and first results, *Atmos. Chem. Phys.*, 10, 5191–5212, doi:10.5194/acp-10-5191-2010, 2010.
- Jaffe, D. A. and Wigder, N. L.: Ozone production from wildfires: A critical review, *Atmos. Environ.*, 51, 1–10, 2012.
- Johnson, T. J., Masiello, T., and Sharpe, S. W.: The quantitative infrared and NIR spectrum of CH<sub>2</sub>I<sub>2</sub> vapor: vibrational assignments and potential for atmospheric monitoring, *Atmos. Chem. Phys.*, 6, 2581–2591, doi:10.5194/acp-6-2581-2006, 2006.
- Johnson, T. J., Profeta, L. T. M., Sams, R. L., Griffith, D. W. T., and Yokelson, R. J.: An infrared spectral database for detection of gases emitted by biomass burning, *Vib. Spectrosc.*, 53, 97–102, 2010.
- Jost, C., Trentmann, J., Sprung, D., Andreae, M. O., McQuaid, J. B., and Barjat, H.: Trace gas chemistry in a young biomass burning plume over Namibia: observations and model simulations, *J. Geophys. Res.*, 108, 8482, doi:10.1029/2002JD002431, 2003.
- Karl, T. G., Christian, T. J., Yokelson, R. J., Artaxo, P., Hao, W. M., and Guenther, A.: The Tropical Forest and Fire Emissions Experiment: method evaluation of volatile organic compound emissions measured by PTR-MS, FTIR, and GC from tropical biomass burning, *Atmos. Chem. Phys.*, 7, 5883–5897, doi:10.5194/acp-7-5883-2007, 2007.
- Keeley, J. E., Aplet, G. H., Christensen, N. L., Conard, S. G., Johnson, E. A., Omi, P. N., Peterson, D. L., and Swetnam, T. W.: Ecological foundations for fire management in North American Forest and shrubland ecosystems, General Technical Report PNW-GTR-779, Portland: US Forest Service, 2009.
- Keene, W. C., Lobert, J. M., Crutzen, P. J., Maben, J. R., Scharffe, D. H., Landmann, T., Hely, C., and Brain, C.: Emissions of major gaseous and particulate species during experimental burns of southern African biomass, *J. Geophys. Res.*, 111, D04301, doi:10.1029/2005jd006319, 2006.
- Korontzi, S., Ward, D. E., Susott, R. A., Yokelson, R. J., Justice, C. O., Hobbs, P. V., Smithwick, E. A. H., and Hao, W. M.: Seasonal variation and ecosystem dependence of emission factors for selected trace gases and PM<sub>2.5</sub> for southern African savanna fires, *J. Geophys. Res.*, 108, 4758, doi:10.1029/2003JD003730, 2003.
- Lane, P. N. J., Sheridan, G. J., Noske, P. J., and Sherwin, C. B.: Phosphorus and nitrogen exports from SE Australian forests following wildfire, *J. Hydrol.*, 361, 186–198, doi:10.1016/J.JHYDROL.2008.07.041, 2008.
- Lapina, K., Honrath, R. E., Owen, R. C., Val Martin, M., and Pfister, G.: Evidence of significant large-scale impacts of boreal fires on ozone levels in the midlatitude Northern Hemisphere free troposphere, *Geophys. Res. Lett.*, 33, L10815, doi:10.1029/2006GL025878, 2006.
- Lee, A., Goldstein, A. H., Kroll, J. H., Ng, N. L., Varutbangkul, V., Flagan, R. C., and Seinfeld, J. H.: Gas-phase products and secondary aerosol yields from the photooxida-

- tion of 16 different terpenes, *J. Geophys. Res.*, 111, D17305, doi:10.1029/2006JD007050, 2006.
- Lee S., Liu, W., Wang, Y., Russell, A., and Edgerton, E. S.: Source Apportionments of PM<sub>2.5</sub>: Comparing PMF and CMB Results for 4 Southeast US Sites, *Atmos. Environ.*, 42, 4126–4137, 2008.
- Lenschow, D., Paluch, I., Bandy, A., Thornton, D., Blake, D., and Simpson, I.: Use of a mixed-layer model to estimate dimethylsulfide flux and application to other trace gas fluxes, *J. Geophys. Res.*, 104, 16275–16295, doi:10.1029/1998JD100090, 1999.
- Li, Q., Jacob, D. J., Yantosca, R. M., Heald, C. L., Singh, H. B., Koike, M., Zhao, Y., Sachse, G. W., and Streets, D. G.: A global three-dimensional model analysis of the atmospheric budgets of HCN and CH<sub>3</sub>CN: Constraints from aircraft and ground measurements, *J. Geophys. Res.*, 108, 8827, doi:10.1029/2002JD003075, 2003.
- Liu, Y., Goodrick, S., Achtemeier, G., Jackson, W., Qu, J., and Wang, W.: Smoke incursions into urban areas: simulation of a Georgia prescribed burn, *Int. J. Wildland Fire*, 18, 336–348, 2009.
- Lobert, J. M., Scharffe, D. H., Hao, W. M., Kuhlbusch, T. A., Seuwen, R., Warneck, P., and Crutzen, P. J.: Experimental evaluation of biomass burning emissions: Nitrogen and carbon containing compounds, in: *Global Biomass Burning: Atmospheric, Climatic and Biospheric Implications*, edited by: Levine, J. S., 289–304, MIT Press, Cambridge, Mass., 1991.
- Maksymiuk, C. S., Gayatri, C., Gil, R. R., and Donahue, N. M.: Secondary organic aerosol formation from multiphase oxidation of limonene by ozone: mechanistic constraints via two dimensional heteronuclear NMR spectroscopy, *Phys. Chem. Chem. Phys.*, 11, 7810–7818, doi:10.1039/b820005j, 2009.
- Mason, S. A., Field, R. J., Yokelson, R. J., Kochivar, M. A., Tinsley, M. R., Ward, D. E., and Hao, W. M.: Complex effects arising in smoke plume simulations due to inclusion of direct emissions of oxygenated organic species from biomass combustion, *J. Geophys. Res.*, 106, 12527–12539, 2001.
- McMeeking, G. R., Kreidenweis, S. M., Lunden, M., Carrillo, J., Carrico, C. M., Lee, T., Herckes, P., Engling, G., Day, D. E., Hand, J., Brown, N., Malm, W. C., and Collett Jr., J. L.: Smoke-impacted regional haze in California during the summer of 2002, *Agr. Forest Meteorol.*, 137, 25–42, 2006.
- McMeeking, G. R., Kreidenweis, S. M., Baker, S., Carrico, C. M., Chow, J. C., Collett Jr., J. L., Hao, W. M., Holden, A. S., Kirchstetter, T. W., Malm, W. C., and Moosmuller, H.: Emissions of trace gases and aerosols during the open combustion of biomass in the laboratory, *J. Geophys. Res.*, 114, D19210, doi:10.1029/2009JD011836, 2009.
- McMeeking, G. R., Lee, T., Taylor, J. W., Craven, J. S., Burling, I., Sullivan, A. P., Akagi, S., Collett, J. L., Jr., Flynn, M., Coe, H., Urbanski, S., Seinfeld, J. H., Yokelson, R. J., and Kreidenweis, S. M.: Aerosol emissions from prescribed fires in the United States: A synthesis of laboratory and aircraft measurements, *J. Geophys. Res.*, in preparation, 2013.
- Muller, J.-F., Capouet, M., Wallens, S., and Stavrou, T., Vinckier, C., Vankerckhoven, H., Van den Bergh, V., Coeckerberghs, H., Compernelle, F., Peeters, J., Vereecken, L., Fantechi, G., Hermans, I., Coeck, C., Nguyen, T. L., Jacobs, P., Arijs, E., Ameynck, C., and Schoon, N.: Anthropogenic and biogenic influences on the oxidation capacity of the atmosphere, SPSDII Report, Belgian Science Policy Office, 2005.
- Paine, T. D., Blanche, C. A., Nebeker, T. E., and Stephen, F. M.: Composition of loblolly pine resin defenses: comparison of monoterpenes from induced lesion and sapwood resin, *Can. J. For. Res.*, 17, 1202–1206, 1987.
- Pan, X., Underwood, J. S., Xing, J.-H., Mang, S. A., and Nizkorodov, S. A.: Photodegradation of secondary organic aerosol generated from limonene oxidation by ozone studied with chemical ionization mass spectrometry, *Atmos. Chem. Phys.*, 9, 3851–3865, doi:10.5194/acp-9-3851-2009, 2009.
- Park, R. J., Jacob, D. J., and Logan, J. A.: Fire and biofuel contributions to annual mean aerosol mass concentrations in the United States, *Atmos. Environ.*, 41, 7389–7400, 2007.
- Pfister, G. G., Emmons, L. K., Hess, P. G., Honrath, R., Lamarque, J.-F., Val Martin, M., Owen, R. C., Avery, M. A., Browell, E. V., Holloway, J. S., Nedelec, P., Purvis, R., Ryerson, T. B., Sachse, G. W., and Schlager, H.: Ozone production from the 2004 North American boreal fires, *J. Geophys. Res.*, 111, D24S07, doi:10.1029/2006JD007695, 2006.
- Rappold, A. G., Stone, S. L., Cascio, W. E., Neas, L. M., Kilaru, V. J., Carraway, M. S., Szykman, J. J., Ising, A., Cleve, W. E., Meredith, J. T., Vaughan-Batten, H., Deyneka, L., and Devlin, R. B.: Peat bog wild?re smoke exposure in rural North Carolina is associated with cardio-pulmonary emergency department visits assessed through syndromic surveillance, *Environ. Health Perspect.*, 119, 1415–1420, doi:10.1289/ehp.1003206, 2011.
- Reid, J. S., Hobbs, P. V., Ferek, R. J., Martins, J. V., Blake, D. R., Dunlap, M. R., and Lioussé, C.: Physical, chemical, and radiative characteristics of the smoke dominated regional hazes over Brazil, *J. Geophys. Res.*, 103, 32059–32080, 1998.
- Roberts, J. M., Veres, P. R., Cochran, A. K., Warneke, C., Burling, I. R., Yokelson, R. J., Lerner, B., Gilman, J. B., Kuster, W. C., Fall, R., and de Gouw, J.: Isocyanic acid in the atmosphere and its possible link to smoke-related health effects, *P. Natl. Acad. Sci. USA*, 108, 8966–8971, doi:10.1073/pnas.1103352108, 2011.
- Rothman, L. S., Gordon, I. E., Barbe, A., Benner, D. C., Bernath, P. F., Birk, M., Boudon, V., Brown, L. R., Campargue, A., Champion, J. P., Chance, K., Coudert, L. H., Dana, V., Devi, V. M., Fally, S., Flaud, J. M., Gamache, R. R., Goldman, A., Jacquemart, D., Kleiner, I., Lacome, N., Lafferty, W. J., Mandin, J. Y., Massie, S. T., Mikhailenko, S. N., Miller, C. E., Moazzen-Ahmadi, N., Naumenko, O. V., Nikitin, A. V., Orphal, J., Perevalov, V. I., Perrin, A., Predoi-Cross, A., Rinsland, C. P., Rotger, M., Simecková, M., Smith, M. A. H., Sung, K., Tashkun, S. A., Tennyson, J., Toth, R. A., Vandaele, A. C., and Vander Auwera, J.: The HITRAN 2008 molecular spectroscopic database, *J. Quant. Spectrosc. Ra.*, 110, 533–572, 2009.
- Saathoff, H., Naumann, K.-H., Möhler, O., Jonsson, Å. M., Halquist, M., Kiendler-Scharr, A., Mentel, Th. F., Tillmann, R., and Schurath, U.: Temperature dependence of yields of secondary organic aerosols from the ozonolysis of  $\alpha$ -pinene and limonene, *Atmos. Chem. Phys.*, 9, 1551–1577, doi:10.5194/acp-9-1551-2009, 2009.
- Schiller, C. L., Locquiao, S., Johnson, T. J., and Harris, G. W.: Atmospheric measurements of HONO by tunable diode laser absorption spectroscopy, *J. Atmos. Chem.*, 40, 275–293, 2001.
- Seinfeld, J. H. and Pandis, S. N.: *Atmospheric Chemistry and Physics – From Air Pollution to Climate Change*, John Wiley & Sons, New York, USA, 1998.

- Simpson, I. J., Akagi, S. K., Barletta, B., Blake, N. J., Choi, Y., Diskin, G. S., Fried, A., Fuelberg, H. E., Meinardi, S., Rowland, F. S., Vay, S. A., Weinheimer, A. J., Wennberg, P. O., Wiebring, P., Wisthaler, A., Yang, M., Yokelson, R. J., and Blake, D. R.: Boreal forest fire emissions in fresh Canadian smoke plumes: C<sub>1</sub>-C<sub>10</sub> volatile organic compounds (VOCs), CO<sub>2</sub>, CO, NO<sub>2</sub>, NO, HCN and CH<sub>3</sub>CN, *Atmos. Chem. Phys.*, 11, 6445–6463, doi:10.5194/acp-11-6445-2011, 2011.
- Singh, H. B., Anderson, B. E., Brune, W. H., Cai, C., Cohen, R. C., Crawford, J. H., Cubison, M. J., Czech, E. P., Emmons, L., and Fuelberg, H. E.: Pollution influences on atmospheric composition and chemistry at high northern latitudes: Boreal and California forest fire emissions, *Atmos. Environ.*, 44, 4553–4564, 2010.
- Spittler, M., Barnes, I., Bejan, I., Brockmann, K. J., Benter, Th., and Wirtz, K.: Reactions of NO<sub>3</sub> radicals with limonene and  $\alpha$ -pinene: Product and SOA formation, *Atmos. Environ.*, 40, 116–127, 2006.
- Stephens, M., Turner, N., and Sandberg, J.: Particle identification by laser-induced incandescence in a solid-state laser cavity, *Appl. Opt.*, 42, 3726–3736, 2003.
- Sudo, K. and Akimoto, H.: Global source attribution of tropospheric ozone: Long-range transport from various source regions, *J. Geophys. Res.*, 112, D12302, doi:10.1029/2006JD007992, 2007.
- Susott, R. A., Olbu, G. J., Baker, S. P., Ward, D. E., Kauffman, J. B., and Shea, R. W.: Carbon, hydrogen, nitrogen, and thermogravimetric analysis of tropical ecosystem biomass, in: *Global Biomass Burning: Atmospheric, Climatic, and Biospheric Implications*, edited by: Levine, J. S., 249–259, MIT Press, Cambridge, MA, 1996.
- Tabazadeh, A., Yokelson, R. J., Singh, H. B., Hobbs, P. V., Crawford, J. H., and Iraci, L. T.: Heterogeneous chemistry involving methanol in tropospheric clouds, *Geophys. Res. Lett.*, 31, L06114, doi:10.1029/2003GL018775, 2004.
- Tereszczuk, K. A., González Abad, G., Clerbaux, C., Hurtmans, D., Coheur, P.-F., and Bernath, P. F.: ACE-FTS measurements of trace species in the characterization of biomass burning plumes, *Atmos. Chem. Phys.*, 11, 12169–12179, doi:10.5194/acp-11-12169-2011, 2011.
- Trentmann, J., Yokelson, R. J., Hobbs, P. V., Winterrath, T., Christian, T. J., Andreae, M. O., and Mason, S. A.: An analysis of the chemical processes in the smoke plume from a savanna fire, *J. Geophys. Res.*, 110, D12301, doi:10.1029/2004JD005628, 2005.
- Turetsky, M. R., Kane, E. S., Harden, J. W., Ottmar, R. D., Manies, K. L., Hoy E., and Kasischke, E. S.: Recent acceleration of biomass burning and carbon losses in Alaskan forests and peatlands, *Nature Geosci.*, 4, 27–31, doi:10.1038/ngeo1027, 2011.
- Val Martín, M., Honrath, R. E., Owen, R. C., Pfister, G., Fialho, P., and Barata, F.: Significant enhancements of nitrogen oxides, black carbon, and ozone in the North Atlantic lower free troposphere resulting from North American boreal wildfires, *J. Geophys. Res.*, 111, D23S60, doi:10.1029/2006JD007530, 2006.
- Vermote, E., Ellicott, E., Dubovik, O., Lapyonok, T., Chin, M., Giglio, L., and Roberts, G.: An approach to measure global biomass burning emissions of organic and black carbon from MODIS fire Radiative power, *J. Geophys. Res.*, 114, D18205, doi:10.1029/2008JD011188, 2009.
- Vrekoussis, M., Kanakidou, M., Mihalopoulos, N., Crutzen, P. J., Lelieveld, J., Perner, D., Berresheim, H., and Baboukas, E.: Role of the NO<sub>3</sub> radicals in oxidation processes in the eastern Mediterranean troposphere during the MINOS campaign, *Atmos. Chem. Phys.*, 4, 169–182, doi:10.5194/acp-4-169-2004, 2004.
- Walser, M. L., Park, J., Gomez, A. L., Russell, A. R., and Nizkorodov, S. A.: Photochemical aging of secondary organic aerosol particles generated from the oxidation of d-limonene, *J. Phys. Chem. A*, 111, 1907–1913, doi:10.1021/jp0662931, 2007.
- Ward, D. E. and Radke, L. F.: Emissions measurements from vegetation fires: A Comparative evaluation of methods and results, *Fire in the Environment: The Ecological, Atmospheric and Climatic Importance of Vegetation Fires*, edited by: Crutzen, P. J. and Goldammer, J. G., John Wiley, New York, 53–76, 1993.
- Weber, R. J., Orsini, D., Daun, Y., Lee, Y.-N., Klotz, P. J., and Brechtel, F.: A Particle-into-Liquid collector for rapid measurement of aerosol bulk chemical composition, *Aerosol Sci. Technol.*, 35, 718–727, 2001.
- Wiedinmyer, C. and Hurteau, M. D.: Prescribed fire as a means of reducing forest carbon emissions in the Western United States, *Environ. Sci. Technol.*, 44, 1926–1932, 2010.
- Wu, S., Mickley, L. J., Jacob, D. J., Logan, J. A., Yantosca, R. M., and Rind, D.: Why are there large differences between models in global budgets of tropospheric ozone?, *J. Geophys. Res.*, 112, D05302, doi:10.1029/2006JD007801, 2007.
- Xu, X., Bingemer, H. G., and Schmidt, U.: The flux of carbonyl sulfide and carbon disulfide between the atmosphere and a spruce forest, *Atmos. Chem. Phys.*, 2, 171–181, doi:10.5194/acp-2-171-2002, 2002.
- Yokelson, R. J., Griffith, D. W. T., Burkholder, J. B., and Ward, D. E.: Accuracy and advantages of synthetic calibration of smoke spectra, in: *Optical Remote Sensing for Environmental and Process Monitoring*, Air Waste Manage. Assoc., Pittsburgh, PA, 365–376, 1996.
- Yokelson, R. J., Ward, D. E., Susott, R. A., Reardon, J., and Griffith, D. W. T.: Emissions from smoldering combustion of biomass measured by open-path Fourier transform infrared spectroscopy, *J. Geophys. Res.*, 102, 18865–18877, 1997.
- Yokelson, R. J., Goode, J. G., Ward, D. E., Susott, R. A., Babbitt, R. E., Wade, D. D., Bertschi, I., Griffith, D. W. T., and Hao, W. M.: Emissions of formaldehyde, acetic acid, methanol, and other trace gases from biomass fires in North Carolina measured by airborne Fourier transform infrared spectroscopy, *J. Geophys. Res.*, 104, 30109–30126, doi:10.1029/1999JD900817, 1999.
- Yokelson, R. J., Christian, T. J., Bertschi, I. T., and Hao, W. M.: Evaluation of adsorption effects on measurements of ammonia, acetic acid, and methanol, *J. Geophys. Res.*, 108, 4649, doi:10.1029/2003JD003549, 2003a.
- Yokelson, R. J., Bertschi, I. T., Christian, T. J., Hobbs, P. V., Ward, D. E., and Hao, W. M.: Trace gas measurements in nascent, aged, and cloud-processed smoke from African savanna fires by airborne Fourier transform infrared spectroscopy (AFTIR), *J. Geophys. Res.*, 108, 8478, doi:10.1029/2002JD002322, 2003b.
- Yokelson, R. J., Karl, T., Artaxo, P., Blake, D. R., Christian, T. J., Griffith, D. W. T., Guenther, A., and Hao, W. M.: The Tropical Forest and Fire Emissions Experiment: overview and airborne fire emission factor measurements, *Atmos. Chem. Phys.*, 7, 5175–5196, doi:10.5194/acp-7-5175-2007, 2007.
- Yokelson, R. J., Christian, T. J., Karl, T. G., and Guenther, A.: The tropical forest and fire emissions experiment: laboratory fire measurements and synthesis of campaign data, *Atmos. Chem. Phys.*, 8, 3509–3527, doi:10.5194/acp-8-3509-2008, 2008.

- Yokelson, R. J., Crounse, J. D., DeCarlo, P. F., Karl, T., Urbanski, S., Atlas, E., Campos, T., Shinozuka, Y., Kapustin, V., Clarke, A. D., Weinheimer, A., Knapp, D. J., Montzka, D. D., Holloway, J., Weibring, P., Flocke, F., Zheng, W., Toohey, D., Wennberg, P. O., Wiedinmyer, C., Mauldin, L., Fried, A., Richter, D., Walega, J., Jimenez, J. L., Adachi, K., Buseck, P. R., Hall, S. R., and Shetter, R.: Emissions from biomass burning in the Yucatan, *Atmos. Chem. Phys.*, 9, 5785–5812, doi:10.5194/acp-9-5785-2009, 2009.
- Yokelson, R. J., Burling, I. R., Urbanski, S. P., Atlas, E. L., Adachi, K., Buseck, P. R., Wiedinmyer, C., Akagi, S. K., Toohey, D. W., and Wold, C. E.: Trace gas and particle emissions from open biomass burning in Mexico, *Atmos. Chem. Phys.*, 11, 6787–6808, doi:10.5194/acp-11-6787-2011, 2011.
- Yokelson, R. J., Burling, I. R., Gilman, J. B., Warneke, C., Stockwell, C. E., de Gouw, J., Akagi, S. K., Urbanski, S. P., Veres, P., Roberts, J. M., Kuster, W. C., Reardon, J., Griffith, D. W. T., Johnson, T. J., Hosseini, S., Miller, J. W., Cocker III, D. R., Jung, H., and Weise, D. R.: Coupling field and laboratory measurements to estimate the emission factors of identified and unidentified trace gases for prescribed fires, *Atmos. Chem. Phys.*, 13, 89–116, doi:10.5194/acp-13-89-2013, 2013.